STRUCTURAL EXAMINATION OF VOLTAGE GATED POTASSIUM CHANNELS BY VOLTAGE CLAMP FLUOROMETRY

by

Moninder Vaid

BSc. University of British Columbia, 2005

A THESIS SUBMITTED IN PARTIAL FULFULLMENT OF THE REQUIREMENTS FOR THE DEGREE OF

MASTER OF SCIENCE

in

THE FACULTY OF GRADUATE STUDIES

(Physiology)

THE UNIVERSITY OF BRITISH COLUMBIA

November 2007

Abstract

Voltage clamp fluorometry (VCF) was first developed in the mid 1990s by Isacoff and his colleagues. In this approach fluorophores are attached to substituted cysteine residues that are engineered by site-directed mutagenesis. Changes in the dielectric environment of the fluorophore report local transitions that are associated with electrically-related and electrically-silent transitions. VCF provides a powerful technique to observe real time reports of ion channel gating conformations. It has proven to be a useful technique because it adds insight that is not available using other techniques. X-ray crystallography studies give a predominantly static picture of the channel, while patch clamping of channels gives information only about residues that effect ionic current flow. Similarly, gating current provides insight only about residues that are charged and move across the membrane electric field.

In this thesis we examined the structural rearrangements of the *Shaker* channel and the effect of 4-AP on channel gating. We also examined for the first time the structural rearrangements of the Kv1.5 gating and the how the channel responds to depolarization pulses. This work is instrumental in the examination of the potassium channel gating.

Table of Contents

List of Figures

List of Abbreviations

Kv	Voltage gates potassium channel
Å	Angstrom
KcsA	Potassium ion channel from *Streptomyces lividans*
MthK	K^+ channel from *Methanobacterium thermoautotrophicum*
VCF	Voltage Clamp Fluorometry
TMRM	Tetramethylrhodamine maleimide
LRET	Lanthanide based energy transfer
FRET	Fluorescence energy transfer
KvAP	Voltage-dependent K+ channel from *Aeropyrum pernix*
Na^+	Sodium ion
hERG	Human ether-a-go-go
HCN	Hyperpolarization-activated cyclic nucleotide-gated cation channel
BK_{Ca}	High Conductance Ca^{+2} activated Potassium Channel
Na^+/K^+ ATPase	Sodium-potassium pump
Na^+/Pi co-transporter	Sodium-phosphate co-transporter
Mg^{+2}	Magnesium ion
CNG	Cyclic nucleotide gated
4-AP	4-aminopyridine
cDNA	Complementary DNA
mM	Millimoles per Liter
ml	Milliliter
mg	Milligram

nl	Nanoliter
ng	Nanogram
°C	Degrees Celsius
nm	Nanometer
μM	Micrometer
W	Watt
kHz	KiloHertz
ms	Millisecond
s	Second
mV	Millivolt
MΩ	Megaohm
M	Moles per liter
τ	Tau
Hz	Hertz
G-V	Conductance versus Voltage relationship
F-V	Fluorescence versus Voltage relationship
MES	Ethyl methyl sulfide
HEPES	4-(2-hydroxyethyl)-1-piperazineethanesulfonic acid
cRNA	RNA derived from cDNA through standard RNA synthesis
NaCl	Sodium chloride
KCl	Potassium chloride
$MgCl_2$	Magnesium chloride
$CaCl_2$	Calcium chloride

$NaHCO_3$	Sodium bicarbonate
$MgSO_4$	Magnesium Sulfate
$Ca(NO_3)_2$	Calcium Nitrate
NaOH	Sodium Hydroxide

Acknowledgements

I would like to thank my supervisor Dr. David Fedida for his guidance over the last two years. He has kept me driven over the last few years to maintain a high quality of work and his encouragement has kept me going through the difficult experimental periods. I would also like to thank my supervisory committee, Dr. Eric Accili and Dr. Steve Kehl, for their input throughout these experiments.

I would also like to make a special thanks to Dr. Thomas Claydon and Dr. Saman Rezazadeh for all their help over the course of this work. Their suggestions, comments, experimental input, and concerns were always appreciated as it allowed the successful completion of several studies. I would like to thank them for their experimental work on both Chapters 2 and 3.

Co-Authorship Statement

The first manuscript chapter entitled 4-aminopyridine prevents the conformational changes associated with P/C-type inactivation in *Shaker* channels was identified and designed by my research supervisor, Dr. David Fedida. I performed all research, data analysis and manuscript preparation.

The second manuscript chapter entitled A novel pore instability in mammalian voltage-gated potassium channels revealed by voltage clamp fluorometry was identified by my supervisor, Dr. David Fedida. I performed all research, data analysis and manuscript preparation.

Chapter 1

Introduction

Ion channels are membrane proteins that span the lipid bilayer and form a pore through which selective ions can pass to alter membrane potential. These proteins are responsible for the passage of ions that allow the propagation of electrical impulses throughout electrically active tissue such as nervous, cardiac and muscle tissue. There are a number of ion channels that conduct and allow for the propagation of action potentials such as sodium, calcium, chloride and potassium channels. Potassium channels are the most diverse ion channels group and defined by their selectivity for potassium over other ions. Voltage gated potassium channels (Kv) channels open in response to changes in membrane voltage which repolarizes the membrane back to the resting membrane potential in many excitable tissues [1-3]. Understanding Kv channel function and structure has physiological importance as these channels directly regulate membrane excitability. The mechanism of channel opening, closing, inactivation and drug block remains unclear and these issues form the basis of this thesis.

Structure of Kv Channels

Kv channels are composed of subunits that tetramerize to form functional channels. Each of the four subunits is composed of six transmembrane domains that combine to form a pore-forming region that allow the flow of potassium ions. The structure of one Kv channel (Kv1.2) has been resolved to 2.9 Å and it suggests that there is a tetrameric arrangement of the subunits around a central pore through which potassium ions can flow down their electrochemical gradient. The structure of Kv1.2 is

shown in Figure 1.1 with each subunit highlighted with a different shade [4]. The crystal structure of Kv1.2 suggests that the transmembrane helices of the channel provide all the elements required for voltage dependent channel gating and the potassium selective pore. The S1-S4 transmembrane helices comprise the structural elements of channel gating and the S5, P-loop and S6 helices form the potassium selective pore.

Activation

Voltage gated channels open and close in response to changes in membrane potential. Kv channels open in response to depolarization which begins with movement of the voltage sensor and results in a conformational change leading to channel opening. Hodgkin and Huxley first suggested the presence of a charged gating particle that reacts to a change in membrane voltage and governs channel activation and inactivation in 1952 [5]. It was not until 1973 that these predicted charged gating particles were recorded. Armstrong and Bezanilla recorded small gating charge currents that were predicted by the movement of gating charges across the membrane [6]. The molecular mechanism of gating charge movement became clearer when voltage gated ion channels were first cloned in the mid-1980s [7-11]. Cloning of these channels revealed that the fourth transmembrane helix contained positively charged amino acids positioned at every third residue. The concentration of these positively charged amino acids suggested that the S4 helix comprised the primary voltage sensor. There are also negatively charged amino acids in the S2 and S3 helices that are thought to have electrostatic interactions with the positively charged residues in S4 [12, 13]. Mutation of these negatively charged residues alters the activation of channels; therefore the S1 to S4 transmembrane helices are

referred to as the voltage-sensing domain. Upon movement of the voltage sensor to the activated position by membrane depolarization, there is a concerted movement that results in channel opening. The precise area of channel opening has been a question of interest for a long period of time and X-ray crystallography has helped to elucidate this matter. There are two crystal structures that when compared help to reveal the mechanism of channel opening. The KcsA crystal structure was crystallized in its closed state [14] and it can be compared with MthK which was crystallized in its open state [15] to reveal the rearrangements associated with channel opening. The two proteins have drastically different structural organization of the M2 transmembrane helix (which is equivalent to the S6 domain of Kv channel) while the outer pore and selectivity filter have very similar structures. The closed and open channels display a drastically different conformation at the cytoplasmic side of the channel. In the closed channel (KcsA), the four subunits constrict near the cytoplasmic side of the channel, referred to as a bundle crossing. This crossing is missing in the MthK channel in which the M2 helices are clearly separated and there is an opening through which ions can pass. The crystal structure of MthK suggests a model of channel opening. According to this model, the M2 helices undergo a conformational change that is dependent on a conserved glycine residue that acts as a hinge to rotate the M2 helices allowing the channel pore to open. In most Kv channels, downstream of the glycine hinge there is a conserved amino acid sequence that is comprised of two proline residues surrounding a hydrophobic residue (referred to as PXP, where X represents the hydrophobic residue). This amino acid sequence introduces a kink in the S6 helix of Kv channels that has been shown to define the intracellular activation gate. Accessibility studies have shown that in the closed state,

residues above the PXP sequence are inaccessible to modification, while residues below are accessible in both the open and closed states [16-19]. Mutation of this conserved sequence affects the ability of the channel to conduct. Mutation of the first proline in *Shaker* causes the channel to by trapped in a permanently closed state and mutation of the second proline locks the channel into a permanently open channel [20]. These results suggest that the PXP domain define the intracellular activation gate and govern the accessibility to the intracellular cavity.

Inactivation

During an extended depolarization Kv channels can undergo conformational changes that render the channel unable to conduct ions. The two forms of inactivation are termed N-type, in which the N-terminus occludes the intracellular channel pore, and P/C-type, in which there are conformational changes in the selectivity filter around the extracellular entrance to the channel and immobilization of the gating charge, both of which prevent ion permeation through the channel. Immobilization refers to a delayed return of gating charge (S4) on repolarization. N-type has been described as the "ball and chain" mechanism in which a series of amino acids at the N-terminus of the channel occludes the intracellular channel pore and prevents ion permeation. Removal of the N-terminus by enzymatic removal or deletion prevents N-type inactivation, but this can be returned by addition of exogenous peptides derived from the N-terminus of the N-type inactivating channel [21-24]. The requirement for N-type inactivation is a series of approximately 10 hydrophobic amino acids followed by a series of amino acids with a net positive charge. Mutation of the hydrophobic residues has a different effect on

inactivation than modification of the charged amino acids. Modification of the charged amino acids alters the binding rate of the inactivation peptide while mutation of the hydrophobic amino acids affects peptide unbinding [24, 25]. Tetrameric K^+ channels can contain multiple inactivation domains although a single inactivation domain is sufficient to confer N-type inactivation [26-28]. N-type is commonly referred to as "fast inactivation" and it underlies a very rapid inactivation process that results in current decay.

Removal of N-type inactivation led to the discovery of a slower form of current inactivation that has been coined C-type inactivation [29]. The underlying mechanism of this slower form of inactivation has been less forthcoming than the fast inactivation (N-type) process. The slower form of inactivation was described as C-type inactivation because the rate of inactivation was dependent on C-terminal *Shaker* splice variants [29]. It is now thought that C-type inactivation is due to conformational changes associated with the selectivity filter and the extracellular entrance of the channel. Several studies have found that C-type inactivation is inhibited by increasing the concentration of extracellular K^+ [21, 30, 31]. The inhibition of C-type inactivation by raising extracellular K^+ has been described as the "foot in the door mechanism" because an ion binding site in the extracellular side of the channel is thought to be occupied, preventing the changes associated with C-type inactivation. The rate of C-type inactivation of *Shaker* channels has been shown to be altered by mutations in the extracellular pore [30]. T449 has been shown to be an important site in the *Shaker* pore and mutagenesis of this residue to tyrosine or valine considerably inhibits the rate of C-type inactivation. Interestingly, the analogous mutations to *Shaker* T449 when made in Kv1.4 to a valine or

tyrosine have a much smaller effect on C-type inactivation in Kv1.4 [32]. Together, these studies have suggested that the rate of C-type inactivation depends on the structure of the outer pore. Nonetheless, mutations of equivalent positions in different channels do not have the same effect on C-type inactivation which suggests that the precise pathway of C-type inactivation may vary depending on the channel studied.

More recently the term P-type inactivation has been used to draw a distinction within C-type inactivation. Loots and Isacoff (1998) [33] used voltage clamp fluorometry to suggest that slow inactivation is the combination of two distinct processes. There is the initial collapse of the channel pore resulting in current decay and a slower conformational change that stabilizes the voltage sensor and pore resulting in charge immobilization. They applied the term P-type inactivation to refer to pore constriction and the term C-type was used to describe the stabilized inactivated conformation after the onset of gating charge immobilization. However, it is difficult to distinguish between pore inactivation and charge immobilization and thus the term P/C type inactivation is often combined to avoid confusion.

Evidence has recently been provided which shows that voltage sensor movement is involved in P/C-type inactivation. The movement of the voltage sensor has been suggested to elicit the conformational rearrangement that results in this slow inactivation process. Direct evidence has been provided by fluorescent probes attached to sites in the voltage sensor and the outer pore that can report on both activation (voltage sensor movement) and inactivation (P/C-type inactivation). Fluorophores conjugated to the extracellular end of S4 at site A359C of *Shaker* have been shown to report on two phases upon depolarization. There is an initial fast phase that is ascribed to voltage sensor

movement and a subsequent slower component with kinetics that occur over the same time scale as inactivation [33, 34]. Analogous observations were made from a fluorescence probe introduced at site S424C in the outer pore of *Shaker*. Site S424C reports on a slow fluorescence change that matches the time course of inactivation and once in this inactivated state, site S424C detects the rapid movements of the voltage sensor. The fluorescence observations therefore indicate that the S4 domain may lie within close proximity to particular regions of the pore. These observations have since been supported by many studies that have attempted to examine the relative location of the S4 to the pore. Several studies have demonstrated disulphide bond formation between cysteine residues substituted in the extracellular end of *Shaker* S4 and S5 segments [35-40]. It has also been suggested that site E418 in *Shaker* may act as an inactivation switch; movement of the voltage sensor breaks a hydrogen bond around residue E418 causing C-type inactivation to occur [41].

As discussed, N-type inactivation can occur if only one N-terminus inactivation domain is present [27, 28]. However, experiments from both *Shaker* and Kv1.3 suggest that C-type inactivation is dependent on all four subunits and is a co-operative transition that results in current decay in the channel [42, 43]. Although the structural mechanisms of N and C-type inactivation are distinct there appears to be an interaction between them. It has been shown that the use-dependent reduction of peak current in *Shaker* was abolished by removal of N-type inactivation or by slowing C-type inactivation [31].

Voltage clamp fluorometry

Voltage clamp fluorometry (VCF) was first developed in the mid 1990s by Isacoff and his colleagues. In this approach fluorophores are attached to substituted cysteine residues that are engineered by site-directed mutagenesis. Changes in the dielectric environment of the fluorophore report local transitions that are associated with electrically-related and electrically-silent transitions. VCF provides a powerful technique to observe real time reports of ion channel gating conformations. It has proven to be a useful technique because it adds insight that is not available using other techniques. X-ray crystallography studies give a predominantly static picture of the channel, while patch clamping of channels gives information only about residues that effect ionic current flow. Similarly, gating current provides insight only about residues that are charged and move across the membrane electric field.

VCF is performed by injecting cRNA of the channel of interest into *Xenopus* oocytes. The cRNA contains point mutations to remove all externally accessible endogenous cysteine residues and insert cysteine residues into regions of interest. When the channel is expressed on the ooctye surface, the oocyte is labelled with TMRM. Two electrode voltage clamp is performed with TMRM bound covalently to the thiol group of the cysteine. The oocyte is placed in the recording chamber above an objective that passes light onto the ooctye and collects the emission from TMRM. A shutter is also employed to selectively pass light onto the ooctye only during protocols in order to avoid bleaching of the fluorophore. If there is a voltage dependent change in the local environment around TMRM then there will be a change in the amount of light energy

being emitted by the fluorophore. The light collected by the objective is then filtered and passed to a photomultiplier tube that quantitates the signal and presents the data in the recording window. This allows the researcher to determine which sites report voltage dependent structural rearrangements and provided insight into channel gating.

The first reported fluorescence reports were recorded from the *Shaker* channel [44]. Tetramethylrhodamine maleimide (TMRM) was attached to cysteine residues in the S3-S4 linker and found to be a faithful reporter of the time and voltage dependence of voltage sensor movement. In addition, fluorophores attached to cysteine residues in the pore were found to report on channel activation and slow inactivation [33, 41, 45]. These reports suggested that there may be a coupling between S4 movement and pore rearrangements, and a mechanistic understanding of slow inactivation was developed from these experiments. Coupling between the S4 helix and the pore was later confirmed by a comprehensive study of the *Shaker* channel in which 37 sites in the pore and voltage sensor were labelled with TMRM [39]. The fluorescence reports from many sites in both the pore and voltage sensor illustrated both a fast and slow component. This suggests that these sites were near enough to report not only on rearrangements occurring in their local environment, but also on coupling that was occurring between the voltage sensor and the pore.

Voltage clamp fluorometry has also been central to our understanding of independence and cooperativity in the rearrangement of the potassium channel voltage sensor. By examining individual subunits in heterotetrameric channels by both gating charge movement and VCF it was shown that the major charge carrying steps occur independently in each subunit while the last cooperative step carries little charge [46].

This discovery was critical for understanding the involvement of S4 movement in channel opening.

Helical Screw Model

A modification of voltage clamp fluorometry has helped to shape our understanding of how the voltage sensor moves charges across the electric field and the absolute distance of S4 movement. In the late 1990s, Bezanilla and Isacoff and their colleagues used LRET (Lanthanide based resonance energy transfer) and FRET (Fluorescence resonance energy transfer) to understand the mechanism of how charge was moved across the electric field. These studies suggested a novel mechanism of voltage sensor movement that was different than the previously proposed sliding model which suggested S4 moved outwards upon depolarization to move the 3 elementary charges per subunit across the membrane [47]. Resonance energy transfer is the interaction between two fluorophores with one acting as a donor and the other as an acceptor to allow an accurate determination of the distance between them. In these studies the researchers placed donors and acceptors between identical residues in the *Shaker* channel S3-S4 linkers and S4 helices to allow for an estimation of changes in subunit distances during activation. Consecutive residues were found to not move in a consistent manner i.e. – all moving closer or all moving further apart. The data suggest that adjacent residues either moved closer together or further away with respect to the equivalent residue in the other subunit. The mechanism that was proposed to explain these as well as previous results was a helical screw model where the S4 helix tilted and underwent a 180° twist during activation, moving the elementary charges across the

electric field [48, 49]. The comprehensive fluorescence study of *Shaker* also provided a confined mechanism of S4 movement that supported the helical screw model [39].

Further LRET and FRET experiments were also performed to understand the distance that S4 moves across the electric field. In the LRET experiments, a donor was placed at sites in the S3-S4 linker and S4 with an acceptor attached to the agitoxin scorpion molecule. Agitoxin has been shown to bind to the external pore either in the open or closed state [50, 51] and does not alter the movement of the voltage sensor. The researchers measured the distances between sites in the voltage sensor and agitoxin under closed and activated conformations of the voltage sensor and found that S4 undergoes a vertical displacement of 2 Å which refuted the large scale translocations suggested from the crystal structure [52]. Support for this conclusion was also provided by a FRET based experiment in which residues in the S4 were labelled with a donor molecule and the acceptor was a lipophilic ion dipicrylamine that distributes itself across the lipid bilayer in a manner that depends on membrane potential. If the S4 segment underwent a transmembrane movement upon depolarization then it was predicted that it would produce a transient fluorescence change. There was no transient fluorescence upon depolarization indicating that S4 does not translocate across the entire lipid bilayer, and suggesting that there is limited transmembrane movement of the voltage sensor [53]. The conclusions drawn from these experiments provide a constraint on voltage sensor movement and therefore add to the controversy of voltage sensor displacement.

Paddle Model

The results from voltage clamp fluorometry disagree with the conclusions drawn by MacKinnon and colleagues from their crystallography work. X-ray crystallography of

the KvAP channel, which is a thermophilic bacterial Kv channel, allowed a clear visualization of the structure of the voltage sensor domain and the pore structure [54, 55]. The pore structure is composed of the S5-P loop-S6 and is surrounded by the S1 and S2 helices. The S3 and S4 helices are situated on the outer perimeter of the channel and the S3 helix, which was thought to exist as a single helix, appeared to be two separate helices that were denoted S3a and S3b. The most surprising aspect of the KvAP crystal structure was the location of the S4 domain, which carries the majority of the gating charge. The S4 helix was found to be near the intracellular membrane and perpendicular to the pore structure. Due to this conformation, the authors proposed a "paddle" model in which the S4 helix translocates across the voltage field to satisfy the experimental data of at least 12 elementary charges crossing the electric field [56]. Using tethered biotin to cysteine residues, the researchers also showed that the S4 or paddle moved a large distance across the membrane (~20 Å), a result that was not easy to reconcile with the previous voltage clamp experiments.

Probing Channel Rearrangements with Voltage Clamp Fluorometry

Much of the more controversial and notable VCF studies have focussed on voltage sensor movement and its coupling to the pore in *Shaker* channels, but many other studies have probed other unclear topics in the ion channel field. VCF has been used to study Na^+, ether-a-go-go K^+, hERG, HCN, BK_{Ca}, Na^+/K^+ ATPase, Na^+/Pi and glutamate channels and (co)transporters. This section will review the literature on the use of voltage clamp fluorometry to study voltage gated channels in order to provide insight into the work attempted in this thesis.

The first study of channels other than the *Shaker* channel was completed in Na^+ channels to understand if the voltage sensors of the different domains had an involvement in the fast inactivation process. The S4's of the different domains were probed with TMRM and the results suggested that domains I and II were not linked to fast inactivation but domains III and IV revealed kinetics that correlated with fast inactivation and charge immobilization. This suggested to the authors that there was a novel mechanism in which voltage sensor movement was linked to inactivation, but only through domains III and IV [57]. Voltage sensor movement of sodium channels was also probed to discover the domains responsible for the different components of gating charge movement [58]. The different S4 domains had kinetics that were similar to different components of gating. The residues in domains I-III had fluorescence that was comparable to the fast component of gating currents while domains IV had fluorescence that correlated with the slow component of gating suggesting that the S4 of domain IV forms a later step in the activation sequence. The authors therefore proposed a novel model of sodium channel activation in which domain III moves first and then domains I and II and then finally domain IV moves to cause channels to open. The initial studies of the voltage gated Na^+ channel with VCF have therefore aided in the understanding of activation and inactivation processes in this channel.

Voltage-gated potassium channels were also further studied in the examination of both the hERG and ether-a-go-go channels. The voltage sensor of hERG channels was studied in an attempt to understand the slow activation and rapidly inactivating gating of the channel [59]. Fluorescence reported both a fast and slow phase, which suggested that the slow activation gating of hERG is produced by slow voltage sensor movement while

the fast phase of fluorescence reported on inactivation gating. However, modification of inactivation did not affect the fluorescence report and suggested that the fast fluorescence report may not be a report on inactivation. The ether-a-go-go K^+ channel was studied to examine the effect of Mg^{+2} and other divalent cations on channel activation [60]. Labelling of the voltage sensor with TMRM reported both fast and slow phases. Mg^{+2} affected the slow phase, but the fast phase representing gating charge current was not modulated. This suggested that Mg^{+2} affected a conformational change of the voltage sensor that was either too small or slow to be detected and helped to explain the effect of Mg^{+2} on eag channel ionic and gating currents.

Larsson and colleagues have begun to examine the HCN channel with VCF. In their first study the mode shift that occurred in HCN channels during prolonged openings was examined [61]. It was thought that the mode shift in HCN channels was due to conformational changes that stabilized the open state of the channel or conformational changes of the voltage sensing domain. Through voltage clamp fluorometry, it was found that fluorescence changes during the mode shift is not simply due to stabilization of the pore domain but that S4 undergoes a slow, lateral movement that causes the observed mode shift. The other study of HCN channels was an attempt to understand how voltage sensor movement triggers channel opening. They found that the S4 undergoes two conformational changes during activation that suggests a multi-state allosteric model for HCN channels that is not compatible with a fast S4 motion. The data suggests that the channel opens after only 2 of the 4 voltage sensing domains of the channel have opened and voltage sensor movement limits channel activation. These

studies have provided novel insight into the action of voltage sensor movement in regulating the function of HCN channels.

Savalli and colleagues examined BK_{Ca} channels with voltage clamp fluorometry to understand the conformational changes that affect the channel during activation [62]. They labelled the S3-S4 linker of the channel with both TMRM and PyMPO and examined the fluorescence and found that the fluorescence had similar voltage dependence to voltage sensor movement and both had a hyperpolarized voltage shift from channel opening. Also, the fluorescence reported both a fast movement (similar to voltage sensor movement) and slow phase, which the authors suggest was the report of a transition between multiple open states. Interestingly, mutation of a tryptophan residue in the S3-S4 linker modified the fluorescence emission from several sites in the linker suggesting that the conformational changes in the linker itself was causing changes in the emission reports. This result is remarkably similar to the report from the *Shaker* channel in which residues in the linker were suggested to cause the quenching observed from other sites in the S3-S4 linker [63]. The group also delved further into the examination of the conformational rearrangements associated with channel opening by labelling sites in the S3-S4 linker and examining the effect of co-expressing the β2 subunit of the BK_{Ca} channel [64] on channel fluorescence. The β2 subunit had previously been shown to modulate channel Ca^{+2} and voltage sensitivity as well as pharmacology and kinetic properties of the channel. The N-terminus of the β2 subunit acts as an inactivating particle to increase the rate of inactivation similar to the fast inactivation process found in Kv channels. The VCF reports did not suggest an enhanced amount of inactivation of the voltage sensor (N-type of inactivation promotes charge immobilization of the voltage

sensor in Kv channels) suggesting that the β2 subunit affects inactivation of the BK_{Ca} channel through a different mechanism than the N-type mechanism of Kv channels. This work was the first study of voltage gated ion channels that showed how fluorescence was modified by an auxillary subunit and allowed the development of a mechanism to explain the change in channel function.

These preliminary studies of voltage-gated ion channels have been instrumental in our attempt to understand the fluorescence reports obtained from the various labelled sites and the processes on which they report. This will aid future researchers by allowing them to study sites that report on specific processes. Several such studies have been recently published. As mentioned modification of channels by auxillary subunits has been studied [64], and comprehensive studies of the *Shaker* channels with pH [65] and 4-AP [34](Chapter 2) have been performed. Since the *Shaker* channel has been thoroughly studied by VCF [33, 39, 41, 45] the authors attempted to understand the effect of pH on channel function. Acidic pH has been shown to increase channel inactivation and reduce peak current so the sites in the S3-S4 linker and site S424C (in the S5-P loop) which report on inactivation were studied by TMRM labelling. When external pH was decreased the fluorescence reported an acceleration in inactivation, similar to that of the ionic current. The amplitude of fluorescence was reversibly lost from the pore suggesting a decrease in open channel probability. The authors concluded that the reduction of macroscopic current was the result of pH stabilization of the closed-inactivated states and an enhancement of P/C type inactivation of the channel. This study as well as the others mentioned have shown that once the fluorescence signals from

voltage clamp fluorometry have been characterized and understood, they can be used to further our understanding of ion channels and the factors that affect their function.

As described, voltage clamp fluorometry, FRET and LRET have been used to probe the outer structure of voltage gated ion channels. However, there have also been several studies examining the cytosolic rearrangements of cyclic nucleotide gated (CNG) channels. Cyclic nucleotides can regulate properties of ion channels independently of kinases by directly binding to the channel and it has been shown that in CNG channels that this binding favours channel opening [66]. In these studies, CNG channels were expressed in *Xenopus* oocytes and inside out patches were pulled and the intracellular region of the channels were labelled by perfusing TMRM into the bath [67, 68]. In the preliminary studies, the researchers attempted to understand the state dependence of fluorescence quenching and to understand the movements of charges or dipolar residues near the fluorophore during CNG channel activation. This allowed the researchers to explore how the C-terminus of CNG channel was affecting channel opening. This may have implications in the understanding of the mechanism of coupling between voltage sensor movement and channel opening in other voltage-dependent channels. To further understand the internal conformational rearrangements of the CNG channel, the group completed quenching experiments to determine distances between residues. Internal cysteine residues were labelled with bimane and tryptophan residues were placed near these residues. Upon channel activation, if the bimane and trypthophan residues came closer together there would be a quenching of the bimane signal and a reduction in the fluorescence intensity. This will allow researchers to determine which residues move closer or further apart when the channel activates [69]. Therefore this technique may be

instrumental in our understanding of the workings of the intracellular activation gate and the residues that are important in channel opening in real time.

Drug Binding

Voltage-gated ion channels are pharmacologically modulated in nature by toxins that have evolved in venomous animals. These evolutionary derived compounds either block the pore or prevent voltage sensor movement to inhibit channel function thereby shutting down the nervous system of both predators and prey. Pharmaceutical companies and researchers have also sought methods to alter voltage-gated channel function in an attempt to treat diseases such as epilepsy, stroke and cardiac arrhythmias.

Researchers have employed various electrophysiological techniques to determine the mechanism of drug block to channels and the location of their binding sites. These methods include altering holding potential, stimulating the channel with a pre-pulse, inactivating the channel with an inactivating pulse, stimulating the channel at different frequencies and pulsing to different membrane voltages [70-74]. These protocols can be studied in different cellular configurations. Whole cell, inside out and outside out patches allow researchers to determine if block occurs from the inside or outside of the channel [72, 74-77]. Chimera studies, site directed mutagenesis and conjugation of unnatural amino acids can be performed to pin point the residues in the channel that are instrumental for drug binding [78-85]. These techniques have been used by a variety of researchers in elucidating the mechanism of channel block.

However, voltage clamp fluorometry is also a valuable tool in understanding drug binding as it reports real time changes around a residue. So unlike site directed mutagenesis, which allows an understanding of the residues responsible for drug binding,

VCF may allow researchers to pin point real time interactions between the drug and regions of the channel or drug effects on electrically silent states.

Conclusion

Voltage clamp fluorometry is a technique that has been recently developed for the examination of ion channel structure and gating. As noted, unlike X-ray crystallography, VCF allows us to study the structure of ion channels in real time as it reports on conformational changes around the TMRM conjugated to an engineered cysteine residue. VCF was originally used to study the *Shaker* potassium channel but the technique has been transferred to several other channels [57-69]. It has been used to further our understanding of a number of ion channels and forms the basis of the work comprising this thesis. We have examined the mechanism of 4-AP block on the well-characterized *Shaker* channel (Chapter 2). Also, we have attempted to understand the fluorescence report from the Kv1.5 ion channel, as this will aid in our understanding of the gating of this important cardiac ion channel and will likely form the basis of future studies (Chapter 3). In the future, VCF is likely to become an integral technique in the study of ion channels, used to advance our understanding of channel structure and function.

Figure 1.1. Crystal structure views of the Kv1.2–ß$_2$ subunit complex. (**A**) Stereoview of a ribbon representation from the side, with the extracellular solution above and the intracellular solution below. Four subunits of the channel (including the T1 domain, voltage sensor, and pore) are colored uniquely. Each subunit of the ß subunit tetramer is colored according to the channel subunit it contacts. The $NADP^+$ cofactor bound to each ß subunit is drawn as black sticks. TM indicates the integral membrane component of the complex. (**B**) Stereoview of a single subunit of the channel and ß subunit viewed from the side. Labels correspond to transmembrane helices (S1 to S6); the Pro-Val-Pro sequence in S6 (PVP); and the N (N) and C (C) termini of the Kv1.2 and ß subunits. The position of the N terminus of the ß subunit, which is located on the side furthest away from the viewer, is indicated by an arrow. (**C**) Stereoview of a ribbon representation viewed from the extracellular side of the pore. Four subunits are colored uniquely.

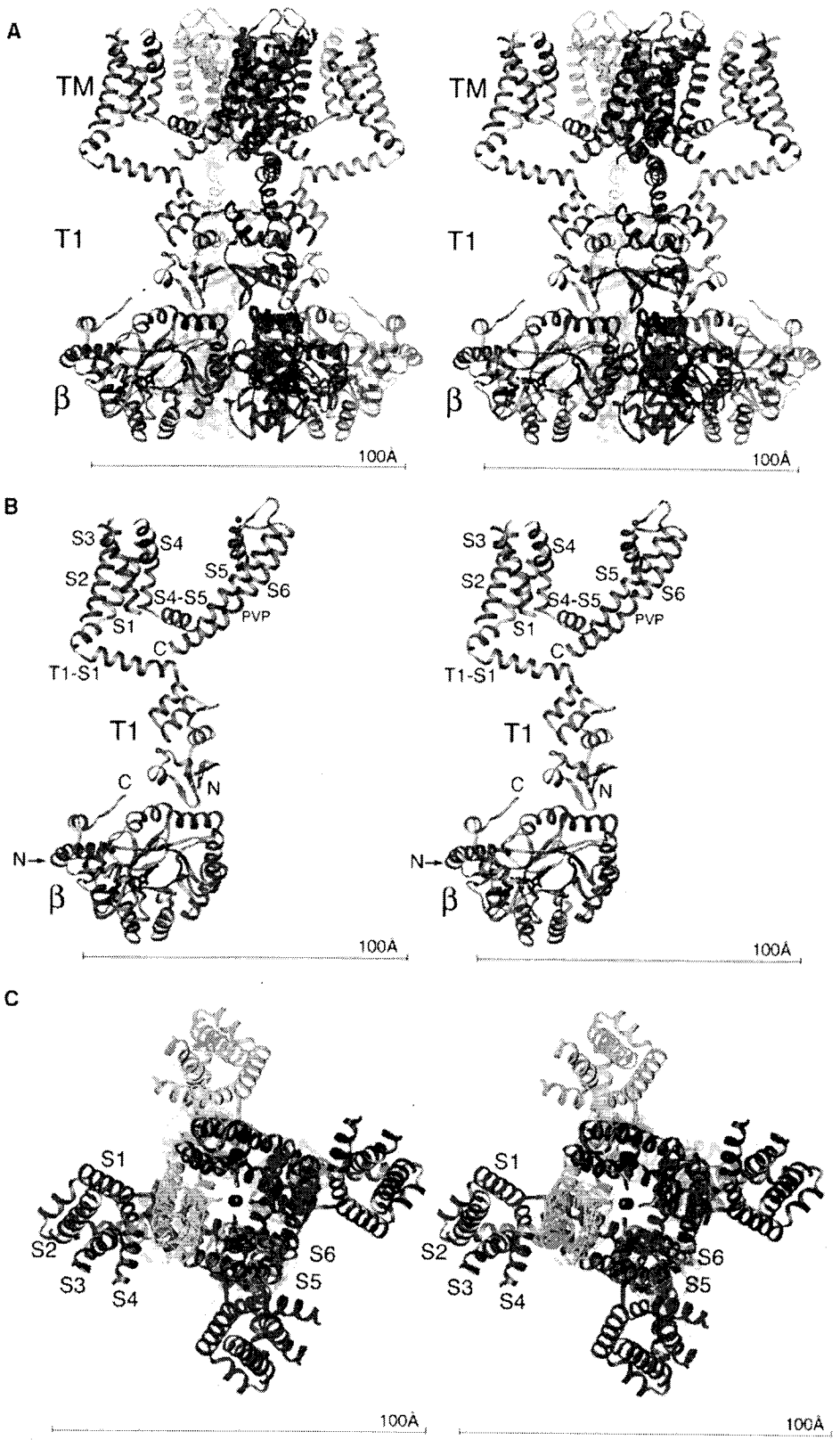
A
TM
T1
β
100Å
TM
T1
β
100Å
B
S3
S4
S2
S5
S6
S4-S5
PVP
S1
C
T1-S1
T1
C
N
N
β
100Å
S3
S4
S2
S5
S6
S4-S5
PVP
S1
C
T1-S1
T1
C
N
N
β
100Å
C
S1
S2
S3
S4
S6
S5
100Å
S1
S2
S3
S4
S6
S5
100Å

References

1. Fedida, D., et al., *Kv1.5 is an important component of repolarizing K+ current in canine atrial myocytes.* Circ Res, 2003. **93**(8): p. 744-51.
2. Wang, Z., B. Fermini, and S. Nattel, *Delayed rectifier outward current and repolarization in human atrial myocytes.* Circ Res, 1993. **73**(2): p. 276-85.
3. Sanguinetti, M.C., et al., *A mechanistic link between an inherited and an acquired cardiac arrhythmia: HERG encodes the IKr potassium channel.* Cell, 1995. **81**(2): p. 299-307.
4. Long, S.B., E.B. Campbell, and R. Mackinnon, *Crystal structure of a mammalian voltage-dependent Shaker family K+ channel.* Science, 2005. **309**(5736): p. 897-903.
5. Hodgkin, A.L. and A.F. Huxley, *A quantitative description of membrane current and its application to conduction and excitation in nerve.* J Physiol, 1952. **117**(4): p. 500-44.
6. Armstrong, C.M. and F. Bezanilla, *Currents related to movement of the gating particles of the sodium channels.* Nature, 1973. **242**(5398): p. 459-61.
7. Timpe, L.C., et al., *Expression of functional potassium channels from Shaker cDNA in Xenopus oocytes.* Nature, 1988. **331**(6152): p. 143-5.
8. Tanabe, T., et al., *Primary structure of the receptor for calcium channel blockers from skeletal muscle.* Nature, 1987. **328**(6128): p. 313-8.
9. Kosower, E.M., *A structural and dynamic molecular model for the sodium channel of Electrophorus electricus.* FEBS Lett, 1985. **182**(2): p. 234-42.

10. Greenblatt, R.E., Y. Blatt, and M. Montal, *The structure of the voltage-sensitive sodium channel. Inferences derived from computer-aided analysis of the Electrophorus electricus channel primary structure.* FEBS Lett, 1985. **193**(2): p. 125-34.

11. Catterall, W.A., et al., *Structure and biosynthesis of neuronal sodium channels.* Ann N Y Acad Sci, 1986. **479**: p. 186-203.

12. Keynes, R.D. and F. Elinder, *The screw-helical voltage gating of ion channels.* Proc Biol Sci, 1999. **266**(1421): p. 843-52.

13. Liu, J., et al., *Negative charges in the transmembrane domains of the HERG K channel are involved in the activation- and deactivation-gating processes.* J Gen Physiol, 2003. **121**(6): p. 599-614.

14. Doyle, D.A., et al., *The structure of the potassium channel: molecular basis of K+ conduction and selectivity.* Science, 1998. **280**(5360): p. 69-77.

15. Jiang, Y., et al., *The open pore conformation of potassium channels.* Nature, 2002. **417**(6888): p. 523-6.

16. Holmgren, M., K.S. Shin, and G. Yellen, *The activation gate of a voltage-gated K+ channel can be trapped in the open state by an intersubunit metal bridge.* Neuron, 1998. **21**(3): p. 617-21.

17. del Camino, D., et al., *Blocker protection in the pore of a voltage-gated K+ channel and its structural implications.* Nature, 2000. **403**(6767): p. 321-5.

18. del Camino, D. and G. Yellen, *Tight steric closure at the intracellular activation gate of a voltage-gated K(+) channel.* Neuron, 2001. **32**(4): p. 649-56.

19. Webster, S.M., et al., *Intracellular gate opening in Shaker K+ channels defined by high-affinity metal bridges.* Nature, 2004. **428**(6985): p. 864-8.

20. Hackos, D.H., T.H. Chang, and K.J. Swartz, *Scanning the intracellular S6 activation gate in the shaker K+ channel.* J Gen Physiol, 2002. **119**(6): p. 521-32.

21. Hoshi, T., W.N. Zagotta, and R.W. Aldrich, *Biophysical and molecular mechanisms of Shaker potassium channel inactivation.* Science, 1990. **250**(4980): p. 533-8.

22. Antz, C., et al., *Control of K+ channel gating by protein phosphorylation: structural switches of the inactivation gate.* Nat Struct Biol, 1999. **6**(2): p. 146-50.

23. Zagotta, W.N., T. Hoshi, and R.W. Aldrich, *Restoration of inactivation in mutants of Shaker potassium channels by a peptide derived from ShB.* Science, 1990. **250**(4980): p. 568-71.

24. Murrell-Lagnado, R.D. and R.W. Aldrich, *Interactions of amino terminal domains of Shaker K channels with a pore blocking site studied with synthetic peptides.* J Gen Physiol, 1993. **102**(6): p. 949-75.

25. Murrell-Lagnado, R.D. and R.W. Aldrich, *Energetics of Shaker K channels block by inactivation peptides.* J Gen Physiol, 1993. **102**(6): p. 977-1003.

26. Gomez-Lagunas, F. and C.M. Armstrong, *Inactivation in ShakerB K+ channels: a test for the number of inactivating particles on each channel.* Biophys J, 1995. **68**(1): p. 89-95.

27. MacKinnon, R., R.W. Aldrich, and A.W. Lee, *Functional stoichiometry of Shaker potassium channel inactivation.* Science, 1993. **262**(5134): p. 757-9.

28. Lee, T.E., L.H. Philipson, and D.J. Nelson, *N-type inactivation in the mammalian Shaker K+ channel Kv1.4.* J Membr Biol, 1996. **151**(3): p. 225-35.

29. Hoshi, T., W.N. Zagotta, and R.W. Aldrich, *Two types of inactivation in Shaker K+ channels: effects of alterations in the carboxy-terminal region.* Neuron, 1991. **7**(4): p. 547-56.

30. Lopez-Barneo, J., et al., *Effects of external cations and mutations in the pore region on C-type inactivation of Shaker potassium channels.* Receptors Channels, 1993. **1**(1): p. 61-71.

31. Baukrowitz, T. and G. Yellen, *Modulation of K+ current by frequency and external [K+]: a tale of two inactivation mechanisms.* Neuron, 1995. **15**(4): p. 951-60.

32. Rasmusson, R.L., et al., *C-type inactivation controls recovery in a fast inactivating cardiac K+ channel (Kv1.4) expressed in Xenopus oocytes.* J Physiol, 1995. **489 (Pt 3)**: p. 709-21.

33. Loots, E. and E.Y. Isacoff, *Protein rearrangements underlying slow inactivation of the Shaker K+ channel.* J Gen Physiol, 1998. **112**(4): p. 377-89.

34. Claydon, T.W., et al., *4-aminopyridine prevents the conformational changes associated with P/C-type inactivation in Shaker channels.* J Pharmacol Exp Ther, 2006.

35. Elinder, F., R. Mannikko, and H.P. Larsson, *S4 charges move close to residues in the pore domain during activation in a K channel.* J Gen Physiol, 2001. **118**(1): p. 1-10.

36. Elinder, F., P. Arhem, and H.P. Larsson, *Localization of the extracellular end of the voltage sensor S4 in a potassium channel.* Biophys J, 2001. **80**(4): p. 1802-9.

37. Elinder, F. and P. Arhem, *Role of individual surface charges of voltage-gated K channels.* Biophys J, 1999. **77**(3): p. 1358-62.

38. Laine, M., et al., *Atomic proximity between S4 segment and pore domain in Shaker potassium channels.* Neuron, 2003. **39**(3): p. 467-81.

39. Gandhi, C.S., E. Loots, and E.Y. Isacoff, *Reconstructing voltage sensor-pore interaction from a fluorescence scan of a voltage-gated K+ channel.* Neuron, 2000. **27**(3): p. 585-95.

40. Gandhi, C.S., et al., *The orientation and molecular movement of a k(+) channel voltage-sensing domain.* Neuron, 2003. **40**(3): p. 515-25.

41. Loots, E. and E.Y. Isacoff, *Molecular coupling of S4 to a K(+) channel's slow inactivation gate.* J Gen Physiol, 2000. **116**(5): p. 623-36.

42. Panyi, G., Z. Sheng, and C. Deutsch, *C-type inactivation of a voltage-gated K+ channel occurs by a cooperative mechanism.* Biophys J, 1995. **69**(3): p. 896-903.

43. Ogielska, E.M., et al., *Cooperative subunit interactions in C-type inactivation of K channels.* Biophys J, 1995. **69**(6): p. 2449-57.

44. Mannuzzu, L.M., M.M. Moronne, and E.Y. Isacoff, *Direct physical measure of conformational rearrangement underlying potassium channel gating.* Science, 1996. **271**(5246): p. 213-6.

45. Cha, A. and F. Bezanilla, *Characterizing voltage-dependent conformational changes in the Shaker K+ channel with fluorescence.* Neuron, 1997. **19**(5): p. 1127-40.

46. Mannuzzu, L.M. and E.Y. Isacoff, *Independence and cooperativity in rearrangements of a potassium channel voltage sensor revealed by single subunit fluorescence.* J Gen Physiol, 2000. **115**(3): p. 257-68.

47. Larsson, H.P., et al., *Transmembrane movement of the shaker K+ channel S4.* Neuron, 1996. **16**(2): p. 387-97.

48. Cha, A., et al., *Atomic scale movement of the voltage-sensing region in a potassium channel measured via spectroscopy.* Nature, 1999. **402**(6763): p. 809-13.

49. Glauner, K.S., et al., *Spectroscopic mapping of voltage sensor movement in the Shaker potassium channel.* Nature, 1999. **402**(6763): p. 813-7.

50. MacKinnon, R. and C. Miller, *Mutant potassium channels with altered binding of charybdotoxin, a pore-blocking peptide inhibitor.* Science, 1989. **245**(4924): p. 1382-5.

51. Goldstein, S.A. and C. Miller, *Mechanism of charybdotoxin block of a voltage-gated K+ channel.* Biophys J, 1993. **65**(4): p. 1613-9.

52. Posson, D.J., et al., *Small vertical movement of a K+ channel voltage sensor measured with luminescence energy transfer.* Nature, 2005. **436**(7052): p. 848-51.

53. Chanda, B., et al., *Gating charge displacement in voltage-gated ion channels involves limited transmembrane movement.* Nature, 2005. **436**(7052): p. 852-6.

54. Jiang, Y., et al., *X-ray structure of a voltage-dependent K+ channel.* Nature, 2003. **423**(6935): p. 33-41.

55. Jiang, Y., et al., *The principle of gating charge movement in a voltage-dependent K+ channel.* Nature, 2003. **423**(6935): p. 42-8.

56. Schoppa, N.E., et al., *The size of gating charge in wild-type and mutant Shaker potassium channels.* Science, 1992. **255**(5052): p. 1712-5.

57. Cha, A., et al., *Voltage sensors in domains III and IV, but not I and II, are immobilized by Na+ channel fast inactivation.* Neuron, 1999. **22**(1): p. 73-87.

58. Chanda, B. and F. Bezanilla, *Tracking voltage-dependent conformational changes in skeletal muscle sodium channel during activation.* J Gen Physiol, 2002. **120**(5): p. 629-45.

59. Smith, P.L. and G. Yellen, *Fast and slow voltage sensor movements in HERG potassium channels.* J Gen Physiol, 2002. **119**(3): p. 275-93.

60. Bannister, J.P., et al., *Optical detection of rate-determining ion-modulated conformational changes of the ether-a-go-go K+ channel voltage sensor.* Proc Natl Acad Sci U S A, 2005. **102**(51): p. 18718-23.

61. Bruening-Wright, A. and H.P. Larsson, *Slow conformational changes of the voltage sensor during the mode shift in hyperpolarization-activated cyclic-nucleotide-gated channels.* J Neurosci, 2007. **27**(2): p. 270-8.

62. Savalli, N., et al., *Voltage-dependent conformational changes in human Ca(2+)- and voltage-activated K(+) channel, revealed by voltage-clamp fluorometry.* Proc Natl Acad Sci U S A, 2006. **103**(33): p. 12619-24.

63. Sorensen, J.B., et al., *Deletion of the S3-S4 linker in the Shaker potassium channel reveals two quenching groups near the outside of S4.* J Gen Physiol, 2000. **115**(2): p. 209-22.

64. Savalli, N., et al., *Modes of operation of the BKCa channel beta2 subunit.* J Gen Physiol, 2007. **130**(1): p. 117-31.

65. Claydon, T.W., et al., *A direct demonstration of closed-state inactivation of K+ channels at low pH.* J Gen Physiol, 2007. **129**(5): p. 437-55.

66. Craven, K.B. and W.N. Zagotta, *CNG AND HCN CHANNELS: Two Peas, One Pod.* Annu Rev Physiol, 2006. **68**: p. 375-401.

67. Zheng, J. and W.N. Zagotta, *Gating rearrangements in cyclic nucleotide-gated channels revealed by patch-clamp fluorometry.* Neuron, 2000. **28**(2): p. 369-74.

68. Zheng, J. and W.N. Zagotta, *Patch-clamp fluorometry recording of conformational rearrangements of ion channels.* Sci STKE, 2003. **2003**(176): p. PL7.

69. Islas, L.D. and W.N. Zagotta, *Short-range molecular rearrangements in ion channels detected by tryptophan quenching of bimane fluorescence.* J Gen Physiol, 2006. **128**(3): p. 337-46.

70. Castle, N.A., et al., *4-Aminopyridine binding and slow inactivation are mutually exclusive in rat Kv1.1 and Shaker potassium channels.* Mol Pharmacol, 1994. **46**(6): p. 1175-81.

71. McCormack, K., W.J. Joiner, and S.H. Heinemann, *A characterization of the activating structural rearrangements in voltage-dependent Shaker K+ channels.* Neuron, 1994. **12**(2): p. 301-15.

72. Choquet, D. and H. Korn, *Mechanism of 4-aminopyridine action on voltage-gated potassium channels in lymphocytes.* J Gen Physiol, 1992. **99**(2): p. 217-40.

73. Yao, J.A. and G.N. Tseng, *Modulation of 4-AP block of a mammalian A-type K channel clone by channel gating and membrane voltage.* Biophys J, 1994. **67**(1): p. 130-42.

74. Bouchard, R. and D. Fedida, *Closed- and open-state binding of 4-aminopyridine to the cloned human potassium channel Kv1.5.* J Pharmacol Exp Ther, 1995. **275**(2): p. 864-76.

75. Kirsch, G.E. and T. Narahashi, *Site of action and active form of aminopyridines in squid axon membranes.* J Pharmacol Exp Ther, 1983. **226**(1): p. 174-9.

76. Kirsch, G.E. and J.A. Drewe, *Gating-dependent mechanism of 4-aminopyridine block in two related potassium channels.* J Gen Physiol, 1993. **102**(5): p. 797-816.

77. Tseng, G.N., M. Jiang, and J.A. Yao, *Reverse use dependence of Kv4.2 blockade by 4-aminopyridine.* J Pharmacol Exp Ther, 1996. **279**(2): p. 865-76.

78. Santarelli, V.P., et al., *A cation-pi interaction discriminates among sodium channels that are either sensitive or resistant to tetrodotoxin block.* J Biol Chem, 2007. **282**(11): p. 8044-51.

79. Caballero, R., et al., *Putative binding sites for benzocaine on a human cardiac cloned channel (Kv1.5).* Cardiovasc Res, 2002. **56**(1): p. 104-17.

80. Decher, N., et al., *Novel KChIP2 isoforms increase functional diversity of transient outward potassium currents.* J Physiol, 2004. **557**(Pt 3): p. 761-72.

81. Herrera, G.M., et al., *Negative feedback regulation of nerve-mediated contractions by KCa channels in mouse urinary bladder smooth muscle.* Am J Physiol Regul Integr Comp Physiol, 2005. **289**(2): p. R402-R409.

82. Franqueza, L., et al., *Molecular determinants of stereoselective bupivacaine block of hKv1.5 channels.* Circ Res, 1997. **81**(6): p. 1053-64.

83. Choi, K.L., et al., *The internal quaternary ammonium receptor site of Shaker potassium channels.* Neuron, 1993. **10**(3): p. 533-41.

84. Lopez, G.A., Y.N. Jan, and L.Y. Jan, *Evidence that the S6 segment of the Shaker voltage-gated K+ channel comprises part of the pore.* Nature, 1994. **367**(6459): p. 179-82.

85. Swartz, K.J. and R. MacKinnon, *Mapping the receptor site for hanatoxin, a gating modifier of voltage-dependent K+ channels.* Neuron, 1997. **18**(4): p. 675-82.

Chapter 2[1]

4-aminopyridine prevents the conformational changes associated with P/C-type inactivation in *Shaker* channels

Introduction

4-aminopyridine (4-AP) is a voltage-gated K^+ (Kv) channel blocker that is useful clinically in the treatment of spinal cord injuries [1], and multiple sclerosis. In addition to its therapeutic applications, 4-AP is routinely used to isolate different types of Kv channels expressed in native tissues based on their affinities for the drug [2, 3], and also to study the biophysical properties of cloned Kv channels [4-6]. It is well accepted that 4-AP is an intracellular blocker of Kv channels [4, 7-10], but the mechanism of 4-AP block is complex and the pathways that have been proposed have involved preferential binding to closed [7, 11], open [8, 9, 12-14], and inactivated states of the channel [15]. It is documented that 4-AP cannot access its binding site when the channel is closed (with the exception of Kv4.2 channels where 4-AP binding occurs exclusively in the closed state [10, 16], because channels only show block and unblock after membrane depolarization to potentials that induce significant channel opening [8, 9, 12, 13]. Furthermore, the recovery of ionic currents after 4-AP washout is contingent on channel opening, which suggests that 4-AP becomes trapped in closed channels and prevents their re-opening [4, 6, 8, 9]. A working model of 4-AP binding [17] suggests that the drug displaces the hydrated K^+ that is trapped in the intracellular cavity [18], causing closure of intracellular activation gate.

[1] A version of this chapter will be submitted for publication. 4-aminopyridine prevents the conformational changes associated with P/C type inactivation in *Shaker* channels.

In support of this idea, 4-AP causes very subtle changes in channels on-gating currents [19], but very profound changes in off-gating [9, 12, 19]. Specifically, 4-AP prevents the slowing of charge return that is linked to channel opening, which suggests that 4-AP selectively blocks the concerted opening step in the activation sequence without altering the early independent gating transitions [6, 17, 20]. Further support for this mechanism of action comes from experiments using the *Shaker* ILT mutation, which energetically dissociates the early independent gating transitions from the last concerted opening transition [21, 22]. Figure 2.1B shows a gating scheme [simplified from that of Armstrong and Loboda (2001)] that summarizes these actions of 4-AP on activation gating.

Although the disruption of channel activation by 4-AP has been extensively investigated, as described above, the relationship between 4-AP block and channel inactivation is less well understood. Castle and co-workers [13] used complex voltage clamp protocols to demonstrate that inactivation and 4-AP binding to *Shaker* and Kv1.1 channels were mutually exclusive, but since then, few additional studies have been performed. The recent development of site-directed voltage clamp fluorometry allows the real-time monitoring of conformational changes associated with channel gating that do not result in ionic current [23, 24]. This is accomplished by examining the changes in the emission from fluorescently-labeled residues, brought about by modifications of the fluorophore microenvironment as the channels activate and inactivate [25, 26]. By attaching tetramethylrhodamine-5-maleimide (TMRM) at A359C in the S3-S4 linker and at S424C in the outer pore (Fig. 2.1A), the conformational rearrangements associated with movement of the voltage sensor during activation and of the pore during

inactivation can be directly observed. For example, fluorescence changes from TMRM attached at A359C occur with the same voltage dependence as movement of the voltage sensor charge [23, 24], and the slow fluorescence deflection from TMRM attached at S424C occurs on a similar timescale to slow inactivation and is sensitive to manipulations that alter its rate [26]. Here, we have used this technique to scrutinize directly the effect of 4-AP on slow inactivation of *Shaker* channels. Relevant amino acid sites used in this study are shown in Fig. 2.1A. We show that 4-AP prevents the conformational changes in *Shaker* channels associated with inactivation. Furthermore, we show that 4-AP can bind to P-type inactivated channels and inhibit the onset of C-type inactivation.

Materials and Methods

Solutions and chemicals

Barth's medium contained (in mM) 88 NaCl, 1 KCl, 2.4 $NaHCO_3$, 0.82 $MgSO_4$, 0.33 $Ca(NO_3)_2$, 0.41 $CaCl_2$, 20 HEPES, titrated to pH 7.4 using NaOH. ND96 bath solution contained (in mM): 96 NaCl, 3 KCl, 1 $MgCl_2$, 2 $CaCl_2$, and 5 HEPES, titrated to pH 7.4 using NaOH. TMRM labeling of oocytes was performed in a depolarizing solution that contained (in mM): 98 KCl, 1 $MgCl_2$, 2 $CaCl_2$ and 5 HEPES, titrated to pH 7.4 using KOH, and 5 μM TMRM. Working concentrations of 4-AP were diluted from a 100 mM stock solution made with ND96 solution and titrated to pH 7.4 using NaOH. All chemicals were purchased from Sigma-Aldrich (Mississauga, Ontario).

Molecular biology and RNA preparation

A modified pBluescript SKII oocyte expression vector (pEXO) was used to express the N-terminal deletion mutant *Shaker* Δ6-46 (a kind gift from Dr. A. Sivaprasadarao) that is fast inactivation removed [27] and the pBluescript SKII expression vector was used to express *Shaker* Δ6-46 ILT (a kind gift from Dr. E. Isacoff).

The A359C and S424C mutations were made in the background of a mutation that replaced the only externally accessible cysteine residue, found in the S1-S2 linker, with a valine residue (C245V). This was done to reduce non-specific labeling and to introduce a cysteine residue for site-specific labeling with TMRM in either the S3-S4 linker (A359C) or the outer pore (turret) region (S424C). We use the terms *Shaker* A359C and *Shaker* S424C to describe the *Shaker* Δ6-46 C245V A359C and *Shaker* Δ6-46 C245V S424C mutant channels, respectively, throughout the manuscript. The T449V

mutation in *Shaker* was used to inhibit slow inactivation [28] and the W434F mutation was used to permanently inactivate channels [29, 30]. Point mutations were generated using the Stratagene Quikchange kit (Stratagene, La Jolla, CA). All primers used were synthesized by Sigma Genosys (Oakville, Ontario). All constructs were sequenced using the core facility unit at the University of British Columbia. cDNA was linearized using BstEII (for *Shaker* Δ6-46 channels) or HindIII (for *Shaker* Δ6-46 ILT channels). cRNA was synthesized from linear cDNA using the T7 mMessage mMachine T7 Ultra cRNA transcription kit (Ambion, Austin, TX).

Oocyte preparation and Injection

Xenopus laevis oocytes were prepared and isolated as described previously [31]. Briefly, gravid frogs were terminally anesthetized and stage V-VI oocytes were isolated and defolliculated using a combination of collagenase treatment (1 h in 1 mg/ml collagenase type 1; Sigma-Aldrich) and manual defolliculation. Oocytes were injected with 50 nl (5-10 ng) cRNA using a Drummond digital microdispenser (Fisher Scientific, Ontario, Canada) and then incubated in Barth's medium at 19 °C. Currents were recorded 1-7 days after injection.

Voltage-clamp fluorometry

Labeling of introduced cysteine residues was performed with tetramethylrhodamine-5-maleimide (TMRM, Invitrogen), which reacts specifically with cysteine residues and has a maximum light absorption at 542 nm and a maximum emission at 567 nm. Oocytes were washed and labeled with 50 μM TMRM in oocyte

depolarizing solution for 30 min at 10 °C in the dark. Oocytes were then placed in ND96 solution in the dark until being voltage clamped at room temperature. Fluorometry was performed using a Nikon TE300 inverted microscope with Epi-Fluorescence attachment and a 9412b Electron Tubes photomultiplier tube (PMT) module (Cairn Research, Kent, UK). The TMRM dye was excited by light from a 100 W mercury lamp that was filtered with a 525 nm band pass excitation filter and passed via a dichroic mirror and 20x objective to the oocyte in the bath chamber. Fluorescence emission from the dye was collected via the same 20x objective and filtered through a 565 nm long pass emission filter before being passed to the PMT recording module. Voltage signals from the PMT were then digitized using an Axon Digidata 1322 A/D converter and passed to a computer running pClamp8 software (Axon Instruments, Foster City, CA) to record the fluorescence emission intensity. Fluorescence signals were filtered at 1 kHz with a sampling frequency of 20 kHz (when the pulse duration was 100 ms), 10 kHz (when the pulse duration was 7 s) or 2 kHz (when the pulse duration was 42 s). Traces were not averaged, except for those recorded during 100 ms pulses, which represent the average of five sweeps. To account for the majority of bleaching of the fluorescence signal during 7 or 42 s pulses, the fluorescence recorded during a pulse to -80 mV, where there is no voltage-dependent deflection, was subtracted. Simultaneous voltage clamp of the oocyte and acquisition of the current and voltage signals was achieved using the two-microelectrode voltage clamp technique with a Warner Instruments OC-725C amplifier (Hamden, CT), Axon Digidata 1322 and pClamp8 software. Microelectrodes were filled with 3 M KCl and had a resistance of 0.5-1.5 MΩ.

Data analysis

G-V curves throughout the text were derived using the normalized chord conductance, which was calculated by dividing the maximum current during a depolarizing step by the driving force derived from the K^+ equilibrium potential (internal $[K^+]$ was assumed to be 98 mM). *G-V* curves were fitted with a single Boltzmann function:

$$y = 1/1(1 + \exp(V_{1/2} - V)/k)) \quad (1)$$

where y is the conductance normalized with respect to the maximal conductance, $V_{1/2}$ is the half-activation potential, V is the test voltage and k is the slope factor.

The Hill equation was used to fit the concentration-response relationship of the effect of 4-AP using GraphPad Prism 3.02 (San Diego, CA):

$$y=1/(1+(IC_{50}/[4\text{-AP}])^n) \quad (2)$$

where y is the fraction of current remaining at a given membrane potential, IC_{50} is the concentration required to achieve half maximal block, [4-AP] is the concentration of 4-AP in the bath solution, and n is the Hill coefficient. Data throughout the text and figures are shown as means ± S.E.M.

Results

Shaker A359C TMRM fluorescence can report both channel activation and inactivation

The slow decay of Kv channel current during prolonged depolarizations involves at least two consecutive steps [32, 33], with the first step closing the outer pore (P-type inactivation) and allowing subsequent stabilization of the inactivated state (C-type inactivation), which is reported by stabilization of the activated conformation of the voltage sensor [26, 30, 34-36](also see Fig. 2.1B). Although these processes were first described using standard voltage clamp techniques, changes of channel conformation during P- and C-type inactivation can also be clearly observed using voltage clamp fluorometry [26, 36]. In particular, two sites effectively report the conformational changes occurring during slow inactivation, A359 in the S3-S4 linker, and S424 in the pore. Data in Fig. 2.2A show typical current and fluorescence recordings from *Shaker* A359C channels (Figs. 2.2A and B), and two *Shaker* mutants with disrupted inactivation, T449V (Figs. 2.2D and E) and W434F (Figs. 2.2G and H). Currents are recorded during 100 ms pulses to a range of potentials that activate ionic current; the currents activate rapidly, and at the more positive potentials, decay (inactivate) during the sustained clamp pulse. On the time base studied here, the extent of the decay is small, but clearly seen in comparison to the horizontal dotted line that shows a single exponential fit of the rising phase of current. Fluorescence recordings (Fig. 2.2B) obtained simultaneously with the currents in panel A show a similar rapid onset, here manifested as a decrease in fluorescence, followed at the more positive clamp potentials by a slower declining phase, which corresponds to the current decay seen in Fig. 2.2A. It has been suggested that the

rapid fluorescence decrease reported by A359C represents channel activation, while the slower decay phase reflects channel inactivation [26]. The amplitudes of the fast (F_{fast}) and slow (F_{slow}) phases of the fluorescence report from Fig. 2.2B are plotted together with the activating and inactivating components of the ionic current record, as a function of the potential during the clamp step in Fig. 2.2C. It can be seen that the rapid phase of fluorescence change, F_{fast}, is negatively shifted from the conductance-voltage relation (*G-V*) on the voltage axis as it reports the voltage sensor movement that precedes channel opening [23, 24]. In *Shaker* A359C channels, F_{fast} contributes 64 ± 7 % to the total fluorescence deflection during a 100 ms pulse to +100 mV (n=10). The voltage-dependence of the slow phase of fluorescence deflection, F_{slow}, is displaced to the right of the fast fluorescence relationship, and shows a voltage-dependence similar to that for the *G-V* relation and also the inactivating component of current (I_{inact}), which is a plot of the amplitude of the current that decays during the pulse at each test potential (I_{inact} at each potential is normalized to that at +100 mV). This is expected since inactivation is coupled to channel opening and should approximate the *G-V* relation. F_{slow} contributes 36 ± 7 % to the total fluorescence deflection (n=10). The idea that the slow phase of fluorescence deflection is associated with channel inactivation is supported by experiments on two mutant channels with altered properties of slow inactivation (Fig. 2.2D-2.2I).

The mutation T449V in the outer mouth of the *Shaker* channel pore has long been used to disrupt slow inactivation [28]. Current records in Fig. 2.2D and the voltage relations in Fig. 2.2F show that, as expected, the slow phase of current decay attributable to slow inactivation is largely prevented in this channel (i.e., I_{inact} is absent on this

timescale). Consistent with this, the slow phase of fluorescence decay recorded from A359C is also absent (Fig. 2.2E, 2.2F). A second mutation, W434F, is known to induce permanent P-type inactivation [26, 29, 30, 35], and there are no ionic currents recordable from this mutant (Fig. 2.2G), but the fluorescence report is still robust (Fig. 2.2H), as activation proceeds normally despite the channels being inactivated [29, 35, 37]. It can be seen that although the fast phase of fluorescence is preserved, the slow fluorescence changes are completely abolished (Fig. 2.2H and 2.2I). Taken together, the results in Fig. 2.2 clearly demonstrate that the fluorescence report from A359C can track conformational changes associated with *Shaker* channel activation and of particular importance for the purposes of this study, channel inactivation. Even though channels may be unable to conduct, either before opening, or after inactivation, the fluorophore remains able to report changes in channel gating state.

The effect of 4-AP on channel inactivation

Using voltage-clamp fluorometry, we investigated the effect of 4-AP on the conformational rearrangements associated with channel inactivation by recording ionic currents and fluorescence signals from TMRM attached at A359C during 7 s depolarizing pulses to +60 mV in the absence and presence of 3 mM 4-AP (Fig. 2.3A). In the control trace, channels open rapidly upon depolarization, but then during maintained depolarization the current declines due to the onset of slow (P- then C-type) inactivation. The signal from the fluorophore in the S3-S4 linker (Fig. 2.3A, lower panel) reports on the conformational changes associated with these gating events. On depolarization, there is a rapid fluorescence deflection followed by a slowly declining phase, which displays kinetics similar to the decay of ionic current and represents the transition of channels into

the inactivated conformation as described in Fig. 2.1. This is highlighted in Fig. 2.3B, which shows superimposed traces of ionic current and fluorescence signal decay recorded simultaneously from the same cell. The mean time constants of decay for the ionic current and fluorescence signal from fourteen such experiments are very similar; τ= 2.5 ± 0.2 and τ = 1.9 ± 0.2 s, respectively. On repolarization to the holding potential, the ionic currents rapidly deactivate and channels recover from inactivation. Again, these gating events are reported by the fluorophore (Fig. 2.3C). On repolarization, the fluorescence returns towards baseline and shows a fast phase that has a τ of 87 ± 15 ms and reflects the time course of the return of the voltage sensor during channel deactivation, and a slow phase that has a τ of 739 ± 82 ms, which reflects the slower return of the voltage sensor to its resting state following stabilization of its activated conformation during inactivation [24, 26].

The second site that was labeled to report on inactivation was S424C in the outer pore region. TMRM attached at this site faithfully reports the conformational changes of the pore that are associated with both the onset of and recovery from inactivation [26]. Fig. 2.3D shows ionic currents and fluorescence signals recorded from TMRM-labeled *Shaker* S424C channels. As for *Shaker* A359C, the fluorescence trace in control conditions shows two distinct phases: a fast phase that occurs with a time course similar to activation and which represents 23 ± 2 % of the signal, and a slow phase that occurs with a time course similar to inactivation and which represents 77 ± 2 % of the signal (n=7). Traces in Fig. 2.3E show an overlay of the control current trace and slow fluorescence signal, and illustrates their similar time courses. The τ of ionic current decay was 2.6 ± 0.3 s and that of the fluorescence decay was 3.8 ± 0.9 s (n=14). On

repolarization, the fluorescence signal also shows fast and slow phases. The τ of the fast phase reflecting deactivation is 269 ± 40 ms, and that of the slow phase is 5.2 ± 1.1 s (n=5), which is similar to the time course of the recovery from inactivation (τ = 2.7 ± 0.6 s; n=4).

In the presence of 4-AP, there were marked changes in both the ionic currents and fluorophore reports of both A359C and S424C TMRM-labeled mutant channels. The ionic currents are partially blocked and the rate of the decay is apparently reduced. Peak current is inhibited by 65 ± 6 % at 3 mM 4-AP (n=5). Scaling of the ionic traces in the presence of 4-AP to the control trace in each mutant (the dotted lines in Fig. 2.3A and D) shows that the rate and extent of slow inactivation of ionic current are significantly reduced in the presence of 4-AP. Fluorophore signals during prolonged depolarization recorded in the presence of 4-AP from both channels (Fig. 2.3A and D) show, for the first time, the conformational changes associated with the inactivation of drug bound channels. 4-AP increases the relative contribution of the fast phase of fluorescence change in *Shaker* A359C channels from 39 ± 3 % to 72 ± 5 % and reduces the contribution of slow secondary fluorescence deflection that was associated with channel inactivation from 61 ± 3 % to 28 ± 5 % (n=5; paired t-test, P<0.001). This results in a crossover of the fluorescence traces because 4-AP increases the instantaneous fluorescence deflection by 54 ± 29 %, but reduces the deflection at the end of the depolarizing pulse by 28 ± 9 % (Fig. 2.3A, lower panel). In addition, the fast and slow phases of the return of the fluorescence to baseline on repolarization are markedly accelerated in the presence of 4-AP (Fig. 2.3C). The fast τ is reduced to 40 ± 1 ms (from 87 ± 15 ms without 4-AP) suggesting that deactivation is enhanced, which is consistent

with previous observations that 4-AP abolishes the immobilization of charge return [9, 12, 19], and the slow τ is reduced to 291 ± 21 ms (from 739 ± 82 ms without 4-AP), which is consistent with the view proposed by Castle and co-workers [13] that fewer channels inactivate in the presence of 4-AP during the maintained depolarization. In the case of the *Shaker* S424C channel, the fluorescence signal reporting inactivation is reduced by 64 ± 5 % (n=4) in the presence of 4-AP (Fig. 2.3D, lower panel). An increase in the fast phase is not observed with *Shaker* S424C, probably because the fluorophore at this position does not report as well on activation [26]. Interestingly, the time constants of the fast and slow phases of the return of the fluorescence signal upon repolarization are not different from those in the absence of 4-AP (Fig. 2.3F). The τ of the fast phase is 181 ± 23 ms and that of the slow phase is 6.1 ± 1.0 s (n=5). Taken together, these current and fluorescence data, which allow direct real-time observation of the conformational changes associated with inactivation, confirm that channel inactivation is greatly reduced after 4-AP binding.

To examine the interdependence of 4-AP block and P/C-type channel inactivation further, the effect of 4-AP binding to T449V and W434F channels was examined. Data in Fig. 2.4A show ionic currents and fluorescence signals recorded during 7 s depolarizing pulses to +60 mV from a holding potential of -80 mV. As suggested earlier (Fig. 2.2), the T449V mutation largely prevents inactivation, although some current decay does still persist during a long depolarizing pulse (τ = 4.4 ± 0.7 s and the relative amplitude of the decaying component, a = 0.22 ± 0.03 in *Shaker* T449V A359C compared with τ = 2.5 ± 0.2 s and a = 0.69 ± 0.03 in *Shaker* A359C; n=5; P<0.01, t-test). The reduced inactivation of T449V mutant channels is accompanied by a slowed and

reduced fluorescence decay (τ = 2.4 ± 0.3 s compared with τ = 1.9 ± 0.2 s without the mutation; n=5-16). Similar to *Shaker* A359C channels, 3 mM 4-AP blocked *Shaker* T449V A359C ionic current by 76 ± 2 % (Fig. 2.4A). However, the fluorophore report shows that 4-AP has a much smaller effect on both the fast and slow phases of fluorescence deflection. The extent of the divergence of the fluorescence traces is reduced, because 4-AP increases the instantaneous fluorescence deflection only 21 ± 7 % (compared with 54 ± 29 % in the absence of 4-AP) and reduces the deflection at the end of the pulse by only 13 ± 12 % (compared with 28 ± 9 % in the absence of 4-AP). These data suggest that the reduced inactivation of the T449V mutant diminishes the scope for the effect of 4-AP on the fluorescence signals. The reduction of the small slow fluorescence deflection from *Shaker* T449V A359C in the presence of 4-AP (Fig. 2.4A) is probably due to inhibition of the residual inactivation present in these mutant channels. The fast phase of the fluorescence return of *Shaker* T449V A359C channels is still accelerated by 4-AP, from 43 ± 9 to 9 ± 1 ms (n=3), because 4-AP enhances deactivation, and the τ of the slow phase of the fluorescence return is also reduced from 775 ± 132 to 377 ± 56 ms (n=3). These data show that 4-AP can block currents from inactivation-reduced T449V channels equivalently to A359C channels, and that 4-AP can still inhibit the residual inactivation present in T449V channels although the fluorescence report is much less altered by 4-AP in these channels.

In permanently inactivated W434F channels, ionic currents cannot be recorded (Figs. 2.2G and 2.4C). Despite this, depolarization produces rapid quenching of the large TMRM fluorescence signal from A359C. As described in Fig. 2.2, the fluorophore reports very little secondary slow phase and Fig. 2.4C shows that this is the case even

during 7 s depolarizing pulses. The contribution of the fast phase to the total fluorescence is 95 ± 2 % (Fig. 2.4C). The application of 4-AP has no effect on the kinetics of fluorophore movement during the depolarization except for a small reduction in the absolute signal. In the presence of 3 mM 4-AP, the fast phase contributes 90 ± 4 % to the total deflection (n=3), which is not different from that without 4-AP. As in *Shaker* A359C channels (Fig. 2.3C), 4-AP accelerates the fast phase of the return of the fluorescence signal on repolarization (Fig. 2.4D). The τ of the fast phase is reduced from 49 ± 15 ms in the absence to 23 ± 1 ms in the presence of 3 mM 4-AP (n=3), which is consistent with the previous observation that 4-AP abolishes immobilization of the voltage sensor of W434F channels on repolarization [12]. Although there is no slow secondary fluorescence deflection from W434F channels during a 7 s depolarization, the recovery of the fluorescence signal on repolarization shows a slow phase with a τ of 474 ± 3 ms that likely represents the recovery of channels that become C-type inactivated during the voltage pulse. This is consistent with previous observations that P-type inactivated W434F channels are able to undergo C-type inactivation during prolonged depolarization [35]. Interestingly, 4-AP accelerates the slow phase of fluorescence return on repolarization (Fig. 2.4D). The τ of the slow phase of fluorescence return is reduced to 167 ± 65 ms in the presence of 3 mM 4-AP (n=3). The incomplete return of the fluorescence signal to the baseline in this case may reflect minor bleaching of the signal rather than incomplete voltage sensor return and this is supported by the evidence of similar incomplete fluorescence return observed in other previous records (e.g., Loots and Isacoff, 1998). These data suggest that 4-AP may be able to bind to P-type inactivated channels and inhibit, at least in part, the transition to C-type inactivation.

The onset of 4-AP block detected by changes in Shaker A359C TMRM fluorescence

As described in Fig. 2.3A, 4-AP introduces a crossover of the fluorescence signals from *Shaker* A359C channels in the early stages of a maintained depolarization. To investigate this phenomenon further, we measured the effect of different concentrations of 4-AP on the ionic current and fluorescence report during 200 ms voltage pulses to +60 mV (Fig. 2.5A). In each case in Fig. 2.5A, the control trace in the absence of 4-AP is shown along with the first and fifth pulses (at 0.2 Hz) after a 3 min application of the indicated concentration of 4-AP during which channels were held closed (holding potential -80 mV). It has been shown that block cannot occur until a channel is opened for the first time (first pulse) in the presence of the drug [8, 9, 12]. Steady-state block is reached by the fifth pulse in each case. In the presence of 0.3 mM 4-AP, the peak ionic current amplitude on the first pulse is not different from that of control, but there is a slow decline in the current during the pulse that represents the onset of channel block (Fig. 2.5A, left). The fluorescence signals in Fig. 2.5A accurately report the gating events associated with this onset of channel block. The instantaneous fluorescence signal recorded on the first pulse in the presence of 0.3 mM 4-AP (Fig. 2.5A, right) is identical to that in control conditions, both in terms of amplitude and kinetics, and is followed by a clear decrease of fluorescence that coincides with the decline of ionic current, and saturates once steady-state block is reached by the fifth pulse (Fig. 2.5A, right). Increasing concentrations of 4-AP exaggerate both the decay of the ionic current and the increase of the fluorescence signal (Fig. 2.5A). Since 4-AP does not significantly quench TMRM directly (see Discussion), these data suggest that binding of

4-AP directly increases the fluorescence signal from *Shaker* A359C channels during short depolarizations by inhibiting ongoing inactivation in channels that normally occurs once they open. This allows the fast phase of fluorescence from opening channels to be more completely detected.

Concentration-response curves calculated from steady-state currents at +60 mV, such as those shown in Fig. 2.5A are shown in Fig. 2.5B. 4-AP inhibits ionic current with an IC_{50} of 1.3 ± 0.1 mM and a Hill coefficient, n of 0.92 ± 0.05 (n=3-6). The effect of different concentrations of 4-AP on the steady-state conductance- and fluorescence-voltage relationships is shown in Figs. 2.5C and D. These data are taken from currents and fluorescence reports recorded during 200 ms voltage pulses from -100 to +80 mV. It is clear that increasing the concentration of 4-AP shifts the conductance-voltage relation of *Shaker* A359C channels to more depolarized potentials and also reduces the maximal conductance (Fig. 2.5C). This is consistent with the previous suggestion that 4-AP binding stabilizes the activated-not-open state of the channel [6, 12] where the voltage sensor charges have moved, but the concerted opening step is prevented [20]. In agreement with this, Fig. 2.5D shows that 4-AP has no effect on the $V_{1/2}$ of the fluorescence-voltage relationship suggesting that 4-AP has little effect on voltage sensor movement and that 4-AP bound channels gate normally without significant opening as suggested previously [12, 17]. The fluorescence-voltage relationships also show the concentration-dependent increase in the absolute fluorescence signal amplitude seen in the presence of 4-AP in Figs. 2.3A and 2.5A without any change in the voltage-dependence of the signal. This suggests that the additional fluorescence signal does indeed reflect activation of channels.

4-AP stabilizes the activated-not-open state

The ILT mutant *Shaker* channel provides a useful tool in channel gating studies because it isolates voltage sensor movement from the cooperative opening transition of channels, i.e., a pulse to 0 mV, for example, will move most of the gating charge, but does not culminate in channel opening [21, 22]. This state was recently described as the activated-not-open state [6] and is suggested to be the same state that is stabilized by the binding of 4-AP. We reasoned that the fluorophore report from the ILT mutant channel at 0 mV should therefore be identical to that from 4-AP bound channels and also insensitive to 4-AP. Fig. 2.6A shows current traces and fluorescence signals recorded from *Shaker* ILT A359C channels during a 7 s pulse to 0 mV from a holding potential of -80 mV in the absence and presence of 3 mM 4-AP. Fig. 2.6B shows *G-V* and *F-V* curves plotted from 100 ms pulses over a wide range of potentials. It is clear that at 0 mV, the ILT mutant channels do not open, since there is no observable current, but that the majority of the charge has moved, since the fluorophore reports a rapid and large conformational change. Fig. 2.6B shows that the $V_{1/2}$ of the *G-V* and *F-V* curves of the *Shaker* ILT A359C channel are separated by more than 150 mV and that opening occurs only at very depolarized potentials. The fluorescence report at 0 mV in the absence of 4-AP shows no secondary movement following the conformational changes associated with charge movement (Fig. 2.6A) as it does in the *Shaker* A359C channel in the presence of 4-AP (Fig. 2.3A). Furthermore, 4-AP does not alter the fluorescence report at 0 mV (Fig. 2.6A). The similarity between the fluorophore reports from 4-AP bound channels and the ILT mutant channels is consistent with the idea that 4-AP, like the ILT mutant,

stabilizes the activated-not-open state of the channel. The lack of evidence of an inactivation transition in the fluorescence trace at 0 mV in the absence of 4-AP also supports the argument that inactivation is strictly coupled to opening in this channel.

Discussion

4-AP bound channels cannot inactivate

The fluorescence emission of TMRM attached to A359C in the S3-S4 linker reports a fast decrease, followed by a slower declining phase on depolarization that reflect activation and inactivation gating conformational changes, respectively (Fig. 2.2). It is clear that the report from this position is very sensitive to inactivation gating because a slow fluorescence decay can be observed not only during prolonged depolarization (Fig. 2.3A) when the majority of channels inactivate, but also during short pulses (Fig. 2.2B) when only a small proportion of channels enter the inactivated conformation. We therefore used the fluorescence report from *Shaker* A359C channels to investigate the effect of 4-AP on channel inactivation, because although the effect of 4-AP binding on voltage sensor movement has been extensively studied [9, 12, 17], there is only one report of the effect on inactivation of ionic current, which suggested that inactivation and 4-AP binding are mutually exclusive [13]. Using the secondary slow phase of fluorescence deflection from *Shaker* A359C, as well as the slow report from *Shaker* S424C channels, we have shown directly that 4-AP inhibits the conformational changes associated with inactivation gating of *Shaker* channels (Fig. 2.3). In support of this conclusion, the effect of 4-AP on the slow secondary fluorescence deflection that reflect inactivation was reduced in mutant channels with reduced (T449V; Fig. 2.4A) or permanent (W434F; Fig. 2.4C) inactivation.

Although it is possible that changes in the fluorescence on 4-AP binding are due to inhibition of ion conduction and that K^+ permeation alters the fluorescence report, evidence suggests that this is not the case. 1) On repolarization, ionic current reverses

direction (as seen in Fig. 2.4A), but the fluorescence report does not, as would be expected if ion conduction was the major determinant of the fluorescence signal. 2) Previously, Loots and Isacoff (1998) showed that the rate of the slow fluorescence report is highly dependent on modifications that alter the rate of inactivation of ionic current; for example, low pH enhances inactivation and the fluorescence decay, whereas high K^+ slows inactivation and the fluorescence decay. Consistent with this, the T449V mutation used in the present study (Fig. 2.5A) slows ionic inactivation and reduces the slow fluorescence decay. Taken together, these data suggest that the fluorescence reports in the present study faithfully report activation and inactivation and are not altered by ion permeation. A similar conclusion was reached by Cha and Bezanilla (1997) who demonstrated that TEA and agitoxin block of the pore altered the fluorescence report from A359C but that this was not due to inhibition of ion conduction, rather that the blocking particles prevented conformational changes associated with channel opening.

4-AP can bind to P-type inactivated channels

Using conventional electrophysiology approaches, Castle et al. (1994) showed that 4-AP slows inactivation of Shaker channels and suggests that 4-AP cannot bind inactivated channels. However, it was not possible in these experiments to separate the effects of 4-AP on P-type inactivation from those on C-type inactivation. In the present study, we have directly observed the effect of 4-AP on P-type inactivation by using the W434F permanently P-type-inactivated mutant channel as well as the effect of 4-AP on C-type inactivation by analyzing the return of fluorescence signal to baseline upon repolarization, which represents the extent of stabilization of the voltage sensor in its

activated conformation, a hallmark of C-type inactivation. W434F channels display almost identical gating currents to wild-type channels, they do not conduct K^+ due to permanent P-type inactivation [30]. Despite this, channels are thought to be able to access the C-type inactivated state on depolarization because they still exhibit charge immobilization following maintained depolarization [35]. In the present study, we observed that the return of the fluorescence signal to baseline on repolarization was enhanced in the presence of 4-AP (Fig. 2.4D). These data suggest that 4-AP can bind to P-type inactivated channels and inhibit their progression to the C-type inactivated state. Because 4-AP can only access its binding site in the *Shaker* channel when the intracellular gate is open, these data show that, although W434F channels are permanently inactivated, the intracellular gate opens with similar voltage dependence to that in conducting channels, which is consistent with the previous observation that the tetraethylammonium binding site is also available on depolarization [29]. This conclusion is also consistent with a number of previous studies in which 4-AP is clearly seen to modify gating currents in W434F mutant channels [9, 12, 19]. From this data we cannot determine whether 4-AP can bind to C-type-inactivated channels. If not, this may be consistent with the inability of 4-AP to bind inactivated channels following the very long pulses used by Castle et al. (1994) that presumably drive most channels to the C-type-inactivated state.

Inactivation results in underestimation of voltage sensor movement

When comparing the fluorescence report from *Shaker* A359C in the absence and presence of 4-AP, we observed a prominent crossover early on in the depolarizing pulse

(Fig. 2.3A). This was reflected as an enhancement of the fluorescence signal during 200 ms pulses (Fig. 2.5A) suggesting that 4-AP block resulted in an increased quenching of TMRM during depolarization. However, a number of observations suggest that it is unlikely that the increased amplitude of deflection is due to a non-specific quenching of the TMRM fluorophore by the drug: 1) the basal level of fluorescence emission was the same in the presence and absence of 4-AP, i.e. the increase in the fluorescence signal amplitude only occurs once the channel is opened and 4-AP is allowed to bind; 2) addition of 4-AP to oocytes expressing channels with no accessible external cysteine residue (i.e. *Shaker* Δ6-46 C245V channels) had no effect on fluorophore emission (data not shown); and, 3) emission intensities recorded on excitation of TMRM dye in solution with or without 3 mM 4-AP were not different (data not shown). Instead, we conclude that the increased fluorescence deflection seen during the short pulses in Fig. 2.5A and the crossover of the fluorescence traces in Fig. 2.3A is a consequence of the 4-AP-induced inhibition of inactivation. The peak of the fluorescence trace in the absence of 4-AP is underestimated due to the onset of inactivation, which results in a slow secondary phase of fluorescence. Because 4-AP binding greatly reduces the ability of *Shaker* channels to inactivate, this slow phase is almost abolished resulting in an increase in the amplitude of the fast phase of fluorescence. In support of this conclusion, the slow phase of the fluorescence decay in the presence of 4-AP, and the divergence of the fluorescence trace from that in control conditions, is reduced in the inactivation-deficient T449V mutant (Fig. 2.4A).

4-AP stabilizes the activated-not-open state

It is well established from gating current studies in *Shaker* channels that 4-AP binding does not alter the early independent gating transitions between closed states [12, 17]. Consistent with this, we have shown that the fast fluorescence report from fluorophores attached in the S3-S4 linker at position A359C, is largely unaltered by the binding of 4-AP (Figs. 2.2B and 2.5D). It was recently suggested that, like the ILT mutation, 4-AP promotes the activated-not-open state of the channel [6, 17]. In the present study, the fluorophore report from ILT mutant channels recorded during a maintained depolarization to 0 mV, which activates channels and moves the voltage sensor but does not open channels, mimicked that recorded from normally activating channels in the presence of 4-AP (compare Figs. 2.3A and 2.6A). Furthermore, application of 4-AP did not alter this report (Fig. 2.6). These data support the conclusion that 4-AP binding promotes the activated-not-open channel conformation [6].

Figure 2.1: Relevant sites within the *Shaker* channel and kinetic scheme of 4-AP mechanism of action.

(A) Cartoon structure of the Shaker potassium channel highlight positions of amino acid sites relevant to the present study. The endogenous cysteine residue (C245) in the S1-S2 linker was mutated to a valine to residue. TMRM was attached to sites A359C and S424C in the S3-S4 linker and the outer pore, respectively. W434F and T449V were engineered to modify inactivation. The molecular structures of 4-AP and TMRM are also shown. The structure of 4-AP is 2.4 A wide and 3.6 A in length with the inner vestibule of the pore approximately 12 A wide and a TMRM molecule is 14 A across.

(B) Kinetic scheme of the mechanism of action of 4-AP modified from Armstrong and Loboda (2001). C0 to C4 represent the closed states of the channel, and O represents the open state. Transitions between C0 to C4 represent voltage dependent gating transitions between the closed states and C4 to O (*) represents the voltage dependent final concerted opening. C4 can be considered the activated not open state (del Camino and Yellen, 2005; Pathak et al., 2005). 4-AP only binds when the channel is open and once it is bound, 4-AP strongly transitions the channel to the closed 4-AP bound state (C4,AP). 4-AP bound channels are able to undergo the independent transitions through the closed state (C0,AP to C4,AP), but 4-AP impedes the voltage dependent transition to opening. IP and IC represent the P- and C-type inactivated states, respectively. The dashed arrows reflect that the recovery from inactivation transitions are not known. The ability of 4-AP to bind to P-type inactivated channels (IP to IP,AP)

is demonstrated in this study by the action on W434F mutant channels. The mechanism of unbinding of IP,AP was not addressed in this study so the unbinding transition has been omitted for clarity.

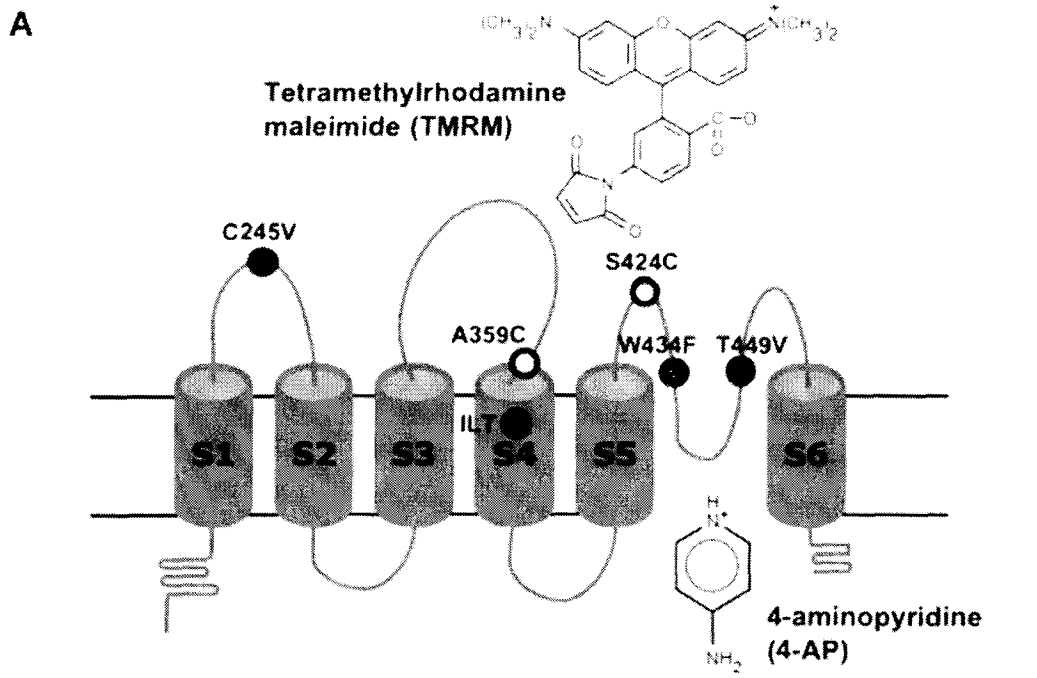
A
Tetramethylrhodamine
maleimide (TMRM)
C245V
S424C
A359C
W434F
T449V
ILT
S1
S2
S3
S4
S5
S6
4-aminopyridine
(4-AP)

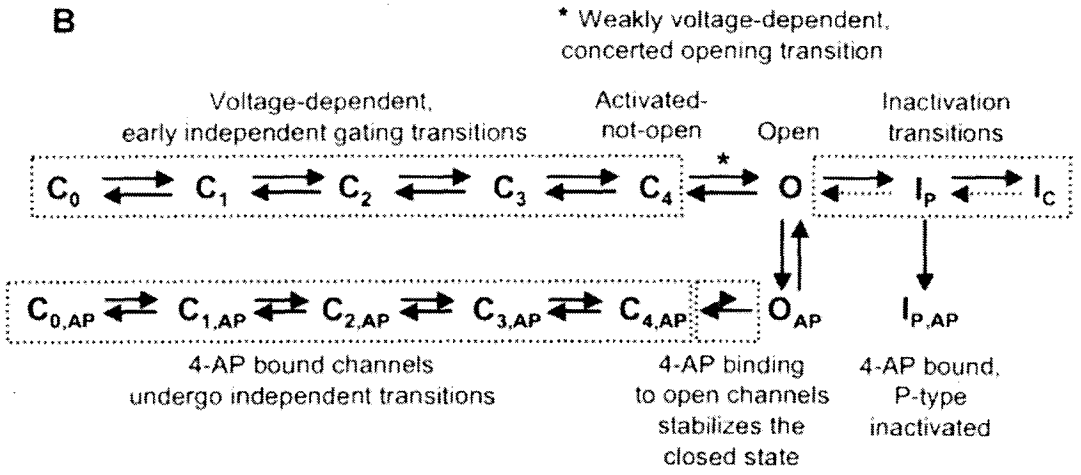
B
* Weakly voltage-dependent, concerted opening transition
Voltage-dependent, early independent gating transitions
Activated-not-open
Open
Inactivation transitions
C0 C1 C2 C3 C4 O IP IC
C0,AP C1,AP C2,AP C3,AP C4,AP OAP IP,AP
4-AP bound channels undergo independent transitions
4-AP binding to open channels stabilizes the closed state
4-AP bound, P-type inactivated

Figure 2.2: TMRM attached to site A359C in Shaker report on both activation and inactivation.
Representative current traces (A, D and G) and fluorescence signals (B, E and H) recorded from Shaker A359C channels without and with mutations T449V (which reduces inactivation) or W434F which permanently inactivates channels (renders them nonconducting) during pulses from -100 to +100 mV from a holding potential of -80 mV. Every other pulse is shown for clarity and dashed lines show extrapolations of exponential fits (from where ~50% of the current has activated) to the time course of ionic current activation (A and D) or the fast component of the fluorescence deflections (B,E and H) at +100 mV to highlight the amount of ionic current and fluorescence decay in each channel. C, F and I, Ffast and Fslow phases of the fluorescence signals and the activating (G-V) and inactivating (Iinact) components of the ionic current record plotted as function of potential (n = 4-10). Iinact represents the amplitude of the current that decays during the 100 ms pulse. The value was normalized to that measured at +100 mV. The fluorescence reports from both Shaker T449V A359C and Shaker W434F A359C channels were fit with a single exponential that represents just that fast phase; therefore Fslow is absent.

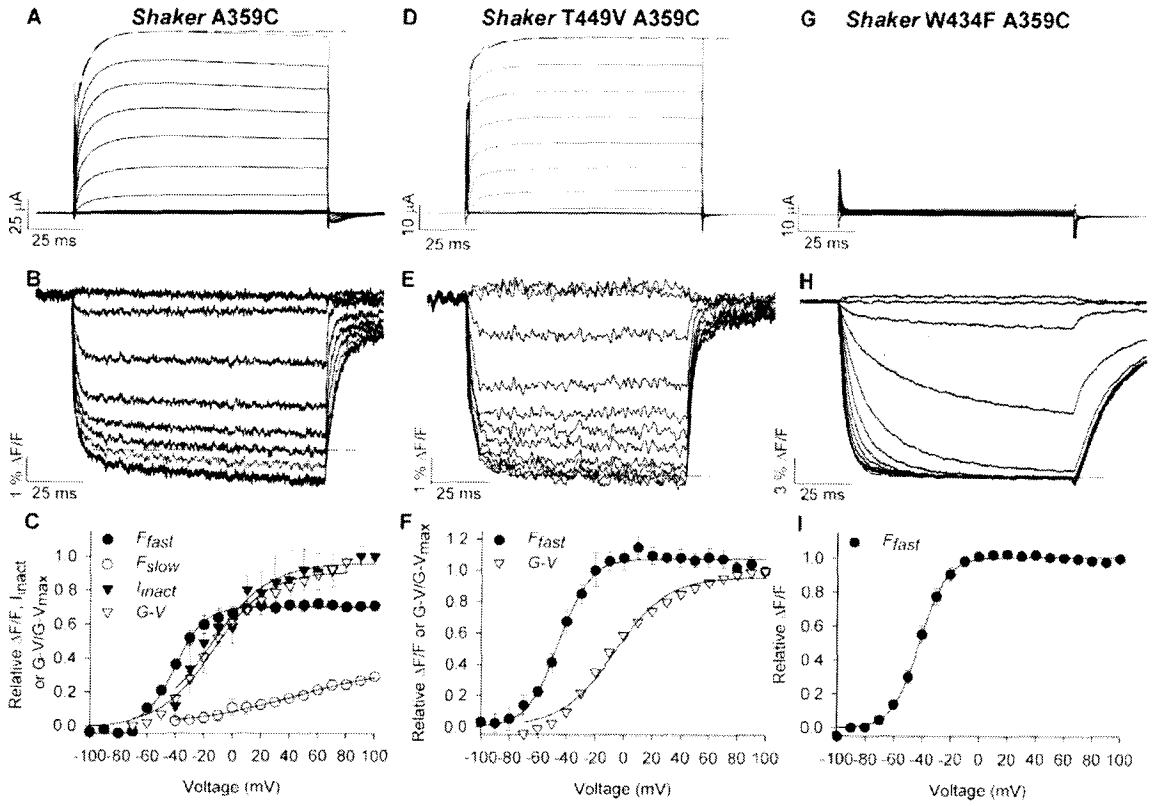
A
Shaker A359C
25 µA
25 ms
B
1 % ΔF/F
25 ms
C
Ffast
Fslow
Imact
G-V
Relative ΔF/F, Imact or G-V/G-Vmax
Voltage (mV)
D
Shaker T449V A359C
10 µA
25 ms
E
1 % ΔF/F
25 ms
F
Ffast
G-V
Relative ΔF/F or G-V/G-Vmax
Voltage (mV)
G
Shaker W434F A359C
10 µA
25 ms
H
3 % ΔF/F
25 ms
I
Ffast
Relative ΔF/F
Voltage (mV)

Figure 2.3: 4-AP removes the inactivation component of fluorescence.
A and D, ionic currents (top) and fluorescence signals (bottom) recorded during a 7 (A) or 42 (D) second depolarization to +60 mV from Shaker A359C (A) or Shaker S424C (D) channels from a holding potential of -80 mV in the absence and presence of 4-AP. The dotted trace represents the normalized ionic current in the presence of 4-AP scaled 2 fold in A and 8 fold in D. B and E, are superimposition of ionic current and the slow phase of the fluorescence deflection in the absence of 4-AP show similar kinetics. The time constants of ionic current and fluorescence signal decay 2.5 +/- 0.2 and 1.9 +/- 0.2 sec, respectively (n=16), for Shaker A359C in B and 2.6 +/-0.3 and 3.8 +/- 0.9 sec, respectively (n = 6 -10), for Shaker S424C in E. C and F, are the normalization of the return of the fluorescence signal to baseline on repolarization in the absence and presence of 4-AP from Shaker A359C (C) and Shaker S424C (F). The return of the fluorescence is biexponential. The fast and slow time constants are 87 +/- 15 (relative amplitude, a = 0.64 +/- 0.07) and 739 +/- 82 ms (a = 0.36 +/- 0.07), respectively, in the absence of 4-AP and 40 +/- 1 (a = 0.75 +/- 0.04) and 291 +/- 21 ms (a = 0.25 +/- 0.04), respectively, in the presence of 3 mM 4-AP in Shaker A359C. The corresponding values in Shaker S424C are 269 +/- 40 ms (a = 0.39 +/- 0.10) and 5.2 +/- 1.1 s (a = 0.61 +/- 0.10) in the absence of 4-AP and 181 +/- 23 ms (a = 0.45 +/- 0.10) and 6.1 +/- 1.0 s (a = 0.55 +/- 0.10) in the presence of 10 mM 4-AP.

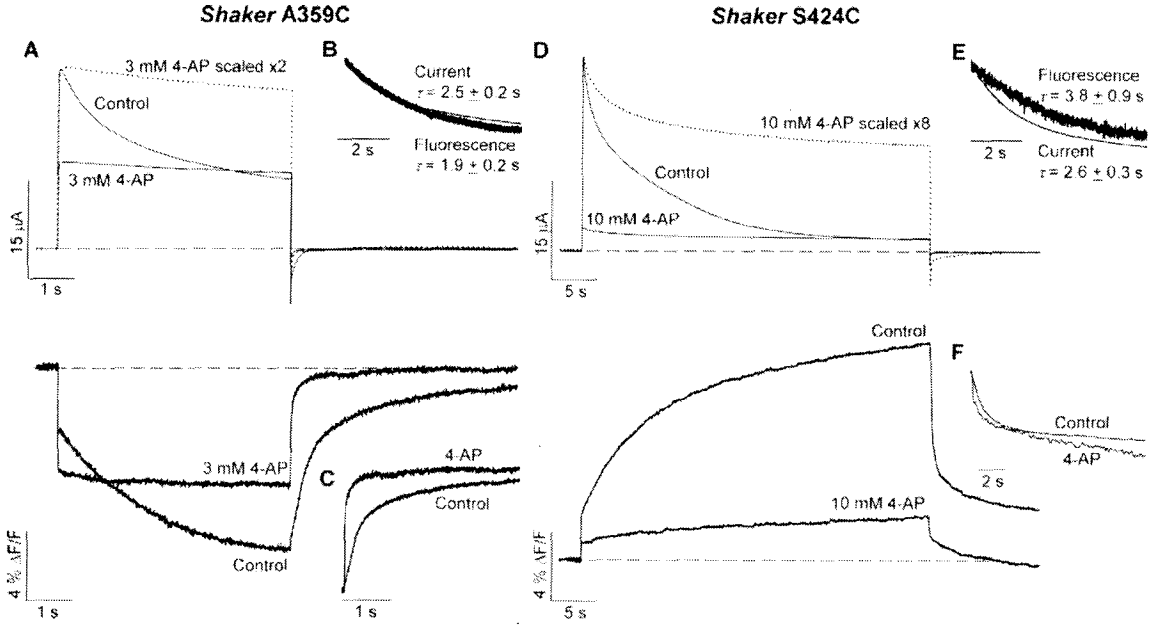
Shaker A359C
Shaker S424C
A
3 mM 4-AP scaled x2
Control
3 mM 4-AP
15 µA
1 s
B
Current
τ = 2.5 ± 0.2 s
2 s
Fluorescence
τ = 1.9 ± 0.2 s
D
10 mM 4-AP scaled x8
Control
10 mM 4-AP
15 µA
5 s
E
Fluorescence
τ = 3.8 ± 0.9 s
2 s
Current
τ = 2.6 ± 0.3 s
3 mM 4-AP
Control
4 % ΔF/F
1 s
C
4-AP
Control
1 s
Control
10 mM 4-AP
4 % ΔF/F
5 s
F
Control
4-AP
2 s

Figure 2.4. Modulation of inactivation alters the effect of 4-AP on *Shaker* A359C TMRM fluorescence.
(A and C) Ionic (top) and fluorescence (bottom) traces recorded from *Shaker* T449V A359C inactivation-reduced mutant channels (A) and *Shaker* W434F A359C permanently inactivated channels (C) during a 7 s depolarizing pulse to +60 mV from a holding potential of -80 mV in the absence and presence of 4-AP. The dotted trace in panel A represents the ionic current in the presence of 4-AP scaled 4-fold to match the peak of the control current. (B and D) Normalization of the return of the fluorescence signal on repolarization in the absence and presence of 4-AP from *Shaker* T449V A359C (B) and *Shaker* W434F A359C (D). The fast and slow time constants are 43 ± 9 (relative amplitude, $a = 0.71 \pm 0.04$) and 775 ± 132 ms ($a = 0.29 \pm 0.04$), respectively, in the absence of 4-AP and 9 ± 1 ms ($a = 0.88 \pm 0.05$) and 337 ± 56 ms ($a = 0.12 \pm 0.05$), respectively, in the presence of 3 mM 4-AP in *Shaker* T449V A359C. The corresponding values in *Shaker* W434F A359C are 49 ± 15 ($a = 0.68 \pm 0.05$) and 474 ± 3 ms ($a = 0.32 \pm 0.05$) in the absence of 4-AP and 23 ± 1 ($a = 0.86 \pm 0.06$) and 167 ± 65 ms ($a = 0.14 \pm 0.06$) in the presence of 3 mM 4-AP.

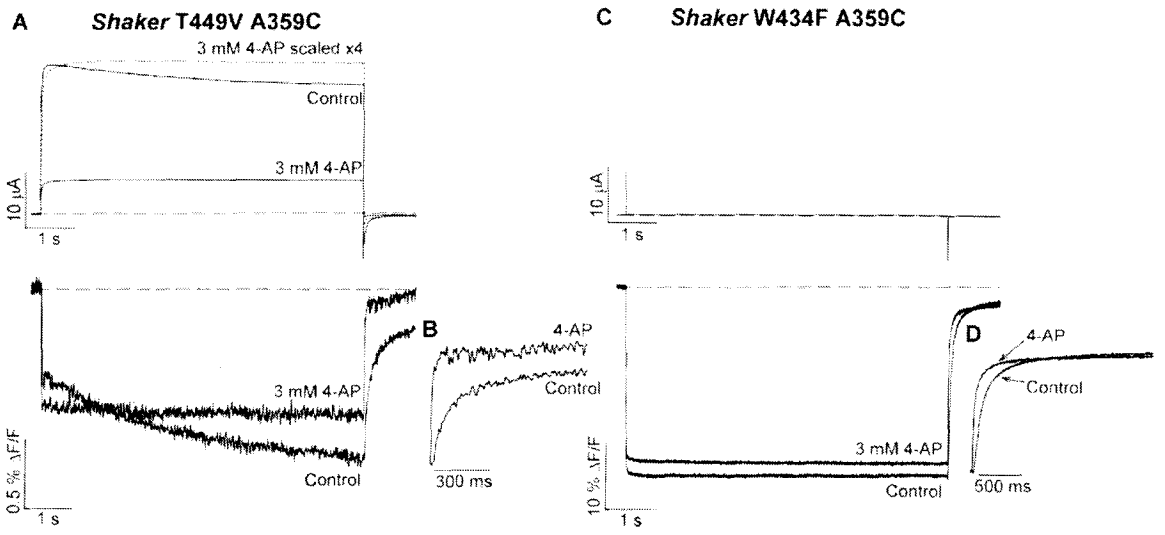
A
Shaker T449V A359C
3 mM 4-AP scaled x4
Control
3 mM 4-AP
10 µA
1 s
3 mM 4-AP
Control
0.5 % ΔF/F
1 s
B
4-AP
Control
300 ms
C
Shaker W434F A359C
10 µA
1 s
D
4-AP
Control
3 mM 4-AP
Control
10 % ΔF/F
1 s
500 ms

Figure 2.5. The onset of 4-AP block detected by changes in *Shaker* A359C TMRM fluorescence.

(A) Ionic currents (left) and fluorescence signals (right) recorded during depolarizing pulses to +60 mV from *Shaker* A359C in the absence of 4-AP (control) and the first and fifth pulses following a 3 min application of 4-AP (the membrane was held at –80 mV during 4-AP application to prevent channel block). (B) 4-AP concentration-response curves generated from the steady-state level of block using ionic currents or fluorescence deflections at +60 mV as shown in panel (A). The IC_{50} and Hill coefficient (n) calculated from the ionic currents are 1.3 ± 0.1 mM and 0.92 ± 0.05, respectively (n=3-6). (C) Conductance-voltage (G-V) relations with increasing concentrations of 4-AP were constructed using the peak current amplitudes during the pulse (n=3-5). $V_{1/2}$ and k values were -10.0 ± 1.8 mV and 20.5 ± 1.5 for control; 3.3 ± 2.6 mV and 26.3 ± 2.0 for 300 μM 4-AP ; 9.7 ± 2.4 mV and 23.9 ± 1.8 for 1 mM 4-AP; 37.9 ± 3.6 mV and 29.0 ± 2.0 for 3 mM 4-AP; 49.3 ± 4.5 mV and 29.1 ± 2.2 for 10 mM 4-AP. These values in the absence of 4-AP are similar to those previously reported for channels with mutations of the S3-S4 linker (Gonzalez et al., 2001) (D) Fluorescence-voltage (F-V) relations were generated by normalizing the peak fluorescence deflections in a given 4-AP concentration to those in the absence of 4-AP in each oocyte (n=3-5). The $V_{1/2}$ and k values were -26.7 ± 1.5 mV and 26.2 ± 1.3, respectively, for control; -35.5 ± 1.7 mV and 23.2 ± 1.4 for 300 μM 4-AP; -39.0 ± 1.1 mV and 19.7 ± 0.9 for 1 mM 4-AP; -38.0 ± 1.3 mV and 18.0 ± 1.1 for 3 mM 4-AP; -26.9 ± 1.8 mV and 24.2 ± 1.5 for 10 mM 4-AP.

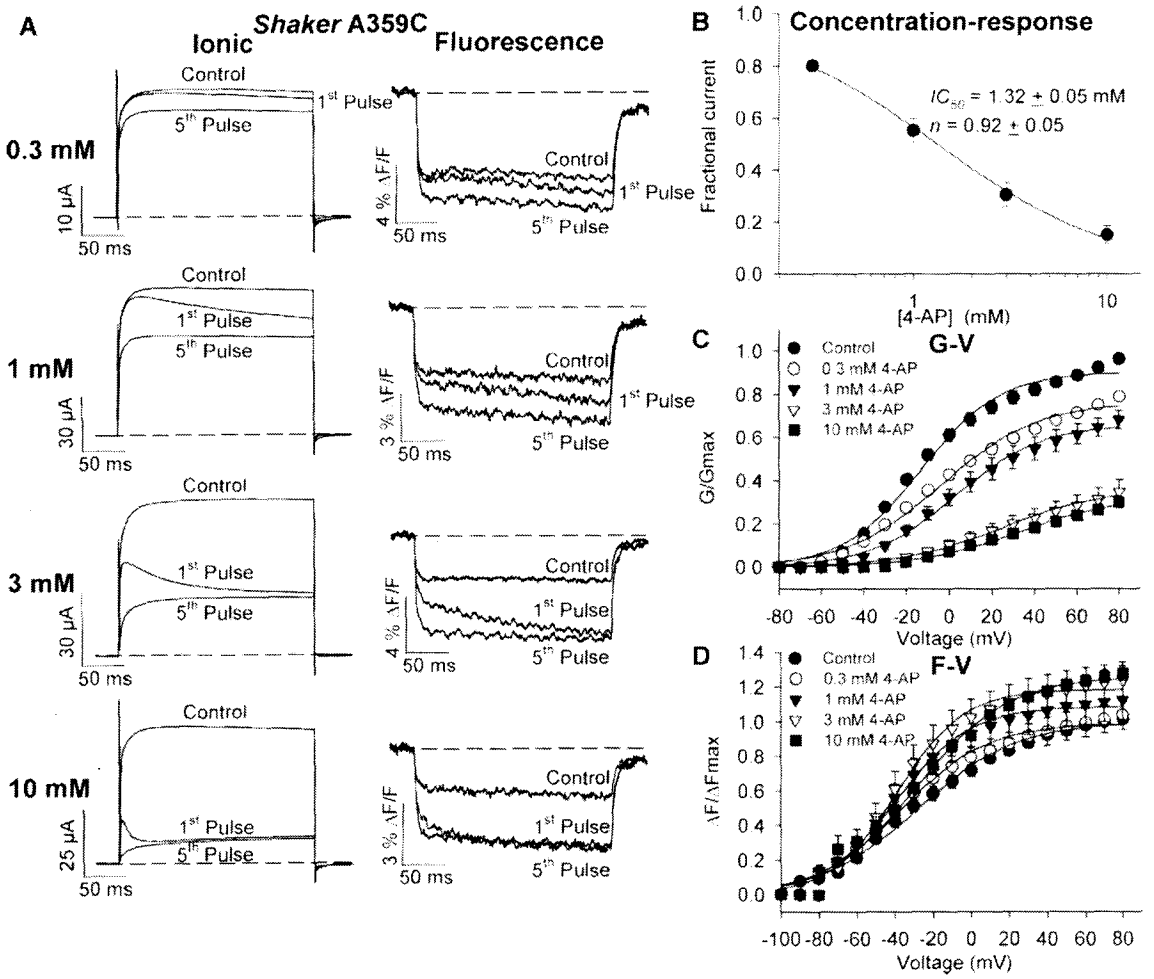
A
Ionic
Shaker A359C
Fluorescence
0.3 mM
1 mM
3 mM
10 mM
Control
1st Pulse
5th Pulse
10 µA
30 µA
25 µA
4 % ΔF/F
3 % ΔF/F
50 ms
B
Concentration-response
Fractional current
IC50 = 1.32 ± 0.05 mM
n = 0.92 ± 0.05
[4-AP] (mM)
C
G-V
0.3 mM 4-AP
1 mM 4-AP
3 mM 4-AP
10 mM 4-AP
G/Gmax
Voltage (mV)
D
F-V
ΔF/ΔFmax
Voltage (mV)

Figure 2.6. 4-AP binding stabilizes the activated-not-open state of the channel. (A) Ionic (top) and fluorescence (bottom) traces recorded from *Shaker* ILT A359C channels in the absence and presence of 3 mM 4-AP during a 7 s depolarizing pulse to 0 mV (where maximum voltage sensor movement takes places without any channel opening) from a holding potential of -80 mV. (B) Isochronal conductance- and fluorescence-voltage relations generated from normalized peak current and fluorescence deflections plotted as a function membrane potential (n=5). $V_{1/2}$ and k values were 101.1 ± 5.4 mV and 36.8 ± 3.5 mV, respectively, for ionic current and the respective values for the fluorescence deflection were -74.5 ± 0.5 mV and 16.1 ± 0.4 mV. The $V_{1/2}$ and k values in the presence of 3 mM 4-AP were 147.6 ± 4.4 mV and 33.4 ± 5.6 mV, respectively, for ionic current and the respective values for the fluorescence deflection were -75.3 ± 0.6 mV and 16.9 ± 0.5 mV.

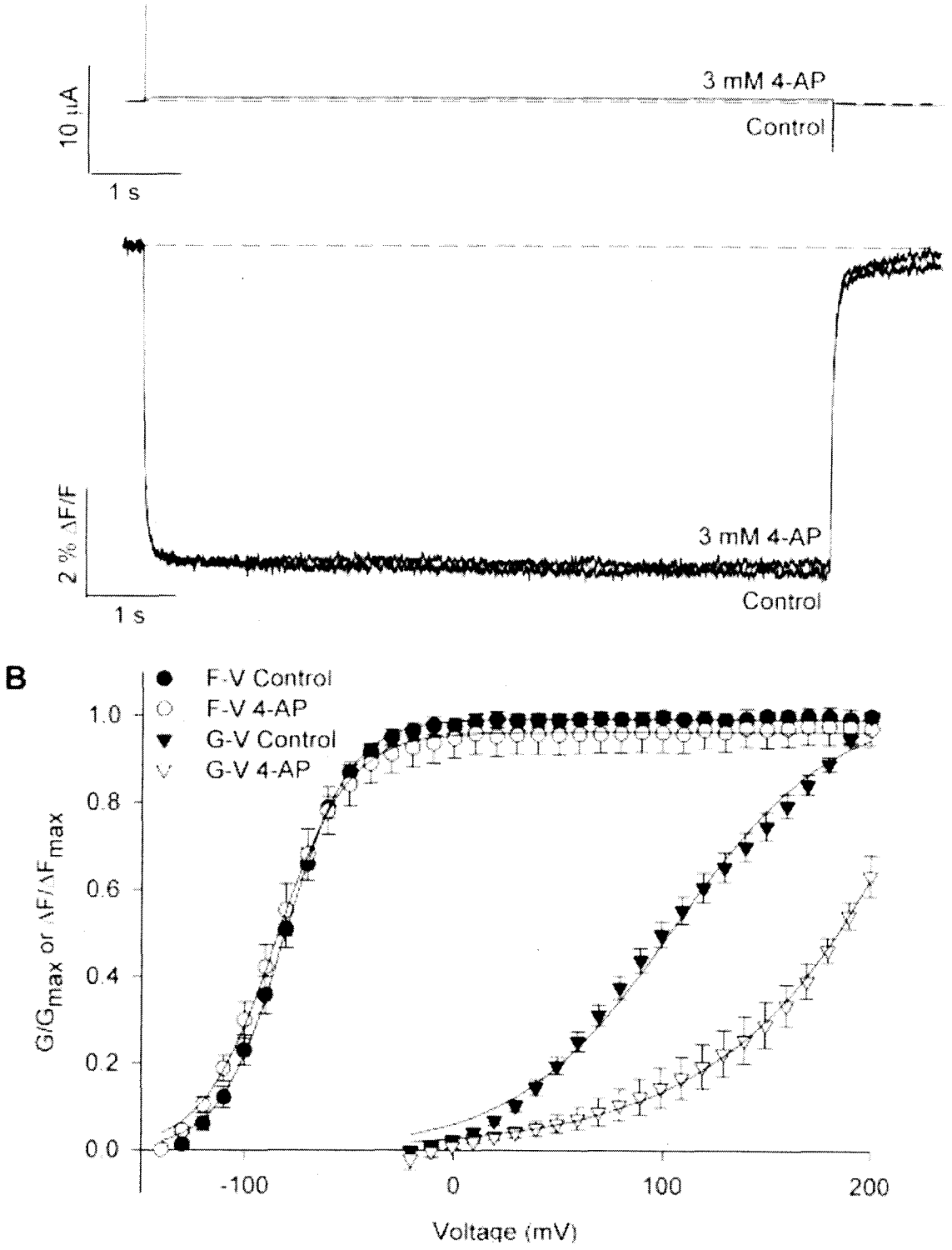
A
Shaker ILT A359C
10 µA
1 s
3 mM 4-AP
Control
2 % ΔF/F
1 s
3 mM 4-AP
Control
B
F-V Control
F-V 4-AP
G-V Control
G-V 4-AP
G/Gmax or ΔF/ΔFmax
1.0
0.8
0.6
0.4
0.2
0.0
-100
0
100
200
Voltage (mV)

References

1. Wolfe, D.L., et al., *Effects of 4-aminopyridine on motor evoked potentials in patients with spinal cord injury: a double-blinded, placebo-controlled crossover trial.* J Neurotrauma, 2001. **18**(8): p. 757-71.
2. Grissmer, S., et al., *Pharmacological characterization of five cloned voltage-gated K+ channels, types Kv1.1, 1.2, 1.3, 1.5, and 3.1, stably expressed in mammalian cell lines.* Mol Pharmacol, 1994. **45**(6): p. 1227-34.
3. Shieh, C.C. and G.E. Kirsch, *Mutational analysis of ion conduction and drug binding sites in the inner mouth of voltage-gated K+ channels.* Biophys J, 1994. **67**(6): p. 2316-25.
4. Kirsch, G.E. and J.A. Drewe, *Gating-dependent mechanism of 4-aminopyridine block in two related potassium channels.* J Gen Physiol, 1993. **102**(5): p. 797-816.
5. Shieh, C.C., K.G. Klemic, and G.E. Kirsch, *Role of transmembrane segment S5 on gating of voltage-dependent K+ channels.* J Gen Physiol, 1997. **109**(6): p. 767-78.
6. del Camino, D., M. Kanevsky, and G. Yellen, *Status of the intracellular gate in the activated-not-open state of shaker K+ channels.* J Gen Physiol, 2005. **126**(5): p. 419-28.
7. Kirsch, G.E. and T. Narahashi, *Site of action and active form of aminopyridines in squid axon membranes.* J Pharmacol Exp Ther, 1983. **226**(1): p. 174-9.
8. Choquet, D. and H. Korn, *Mechanism of 4-aminopyridine action on voltage-gated potassium channels in lymphocytes.* J Gen Physiol, 1992. **99**(2): p. 217-40.

9. Bouchard, R. and D. Fedida, *Closed- and open-state binding of 4-aminopyridine to the cloned human potassium channel Kv1.5.* J Pharmacol Exp Ther, 1995. **275**(2): p. 864-76.

10. Tseng, G.N., M. Jiang, and J.A. Yao, *Reverse use dependence of Kv4.2 blockade by 4-aminopyridine.* J Pharmacol Exp Ther, 1996. **279**(2): p. 865-76.

11. Kirsch, G.E., J.Z. Yeh, and G.S. Oxford, *Modulation of aminopyridine block of potassium currents in squid axon.* Biophys J, 1986. **50**(4): p. 637-44.

12. McCormack, K., W.J. Joiner, and S.H. Heinemann, *A characterization of the activating structural rearrangements in voltage-dependent Shaker K+ channels.* Neuron, 1994. **12**(2): p. 301-15.

13. Castle, N.A., et al., *4-Aminopyridine binding and slow inactivation are mutually exclusive in rat Kv1.1 and Shaker potassium channels.* Mol Pharmacol, 1994. **46**(6): p. 1175-81.

14. Yao, J.A. and G.N. Tseng, *Modulation of 4-AP block of a mammalian A-type K channel clone by channel gating and membrane voltage.* Biophys J, 1994. **67**(1): p. 130-42.

15. Thompson, S., *Aminopyridine block of transient potassium current.* J Gen Physiol, 1982. **80**(1): p. 1-18.

16. Kehl, S.J., *4-Aminopyridine causes a voltage-dependent block of the transient outward K+ current in rat melanotrophs.* J Physiol, 1990. **431**: p. 515-28.

17. Armstrong, C.M. and A. Loboda, *A model for 4-aminopyridine action on K channels: similarities to tetraethylammonium ion action.* Biophys J, 2001. **81**(2): p. 895-904.

18. Ray, E.C. and C. Deutsch, *A trapped intracellular cation modulates K+ channel recovery from slow inactivation.* J Gen Physiol, 2006. **128**(2): p. 203-17.

19. Loboda, A. and C.M. Armstrong, *Resolving the gating charge movement associated with late transitions in K channel activation.* Biophys J, 2001. **81**(2): p. 905-16.

20. Pathak, M., et al., *The cooperative voltage sensor motion that gates a potassium channel.* J Gen Physiol, 2005. **125**(1): p. 57-69.

21. Smith-Maxwell, C.J., J.L. Ledwell, and R.W. Aldrich, *Uncharged S4 residues and cooperativity in voltage-dependent potassium channel activation.* J Gen Physiol, 1998. **111**(3): p. 421-39.

22. Smith-Maxwell, C.J., J.L. Ledwell, and R.W. Aldrich, *Role of the S4 in cooperativity of voltage-dependent potassium channel activation.* J Gen Physiol, 1998. **111**(3): p. 399-420.

23. Mannuzzu, L.M., M.M. Moronne, and E.Y. Isacoff, *Direct physical measure of conformational rearrangement underlying potassium channel gating.* Science, 1996. **271**(5246): p. 213-6.

24. Cha, A. and F. Bezanilla, *Characterizing voltage-dependent conformational changes in the Shaker K+ channel with fluorescence.* Neuron, 1997. **19**(5): p. 1127-40.

25. Bezanilla, F., *Voltage sensor movements.* J Gen Physiol, 2002. **120**(4): p. 465-73.

26. Loots, E. and E.Y. Isacoff, *Protein rearrangements underlying slow inactivation of the Shaker K+ channel.* J Gen Physiol, 1998. **112**(4): p. 377-89.

27. Hoshi, T., W.N. Zagotta, and R.W. Aldrich, *Two types of inactivation in Shaker K+ channels: effects of alterations in the carboxy-terminal region.* Neuron, 1991. **7**(4): p. 547-56.

28. Lopez-Barneo, J., et al., *Effects of external cations and mutations in the pore region on C-type inactivation of Shaker potassium channels.* Receptors Channels, 1993. **1**(1): p. 61-71.

29. Perozo, E., et al., *Gating currents from a nonconducting mutant reveal open-closed conformations in Shaker K+ channels.* Neuron, 1993. **11**(2): p. 353-8.

30. Yang, Y., Y. Yan, and F.J. Sigworth, *How does the W434F mutation block current in Shaker potassium channels?* J Gen Physiol, 1997. **109**(6): p. 779-89.

31. Claydon, T.W., et al., *Inhibition of the K+ channel kv1.4 by acidosis: protonation of an extracellular histidine slows the recovery from N-type inactivation.* J Physiol, 2000. **526 Pt 2**: p. 253-64.

32. Yellen, G., *Premonitions of ion channel gating.* Nat Struct Biol, 1998. **5**(6): p. 421.

33. Kurata, H.T., et al., *Separation of P/C- and U-type inactivation pathways in Kv1.5 potassium channels.* J Physiol, 2005. **568**(Pt 1): p. 31-46.

34. De Biasi, M., et al., *Inactivation determined by a single site in K+ pores.* Pflugers Arch, 1993. **422**(4): p. 354-63.

35. Olcese, R., et al., *Correlation between charge movement and ionic current during slow inactivation in Shaker K+ channels.* J Gen Physiol, 1997. **110**(5): p. 579-89.

36. Loots, E. and E.Y. Isacoff, *Molecular coupling of S4 to a K(+) channel's slow inactivation gate.* J Gen Physiol, 2000. **116**(5): p. 623-36.

37. Starkus, J.G., et al., *Macroscopic Na+ currents in the "Nonconducting" Shaker potassium channel mutant W434F.* J Gen Physiol, 1998. **112**(1): p. 85-93.

Chapter 3[1]

A novel pore instability in mammalian voltage-gated potassium channels revealed by voltage clamp fluorometry

Introduction

Voltage clamp fluorometry (VCF) provides a powerful technique to observe time-resolved reports of ion channel gating conformations that are not possible with traditional electrophysiology. In *Shaker* channels, simultaneous recording of ionic current along with changes in fluorescence emission from TMRM attached in the S3-S4 linker has shown that the fluorescence changes provide a faithful report of the time- and voltage-dependence of voltage sensor movement [1, 2]. Similar fluorescence reports of voltage sensor movement have also been described in hERG, eag and BK_{Ca} potassium channels [3-5].

Interestingly, a number of these fluorescence studies report additional conformational changes that occur following activation of the voltage sensors. These rearrangements reflect transitions that are associated with opening of the channel and/or collapse of the outer pore during inactivation. For example, TMRM attached within the S3-S4 linker of the *Shaker* channel detects not only the independent movement of the voltage sensors, but also conformational rearrangements that are coupled with the concerted opening of the intracellular gate [6]. Furthermore, a number of sites within the S3-S4 linker report the slow collapse of the outer pore that occurs during P-/C-type inactivation [7-9]. In addition, whilst some sites in the S3-S4 linker of BK_{Ca} channels report on the rapid voltage sensor movement during activation, other sites report slower

[1] A version of this chapter will be submitted for publication. A novel pore instability in mammalian voltage-gated potassium channels revealed by voltage clamp fluorometry

rearrangements that may reflect transitions between multiple open states [5]. Also, in hERG channels, slow TMRM emission changes that reflect activation of the voltage sensors are accompanied by a fluorescence report of fast events, which are also observed in gating current measurements [10], and which have similar kinetics and voltage-dependence to channel inactivation and may therefore report structural changes that are coupled to inactivation [3].

In the present study, we provide the first fluorescence reports from mammalian Kv1 channels and show that the fluorescence report from TMRM attached in the S3-S4 linker of Kv1.5 channels revealed unique and complex fluorescence changes despite the homology between *Shaker* and Kv1.5 channels. In addition to the report of voltage sensor movement, the fluorophore in Kv1.5 reports a novel rapid decaying component of fluorescence. We demonstrate that this rapid unquenching represents structural changes associated with a novel pore instability that may be associated with channel inactivation. Blocking the channel with 4-AP (4-aminopyridine), raising external K^+ and mutations that alter opening and inactivation rescued channels from this rapid instability, suggesting that VCF reveals a novel pore instability in Kv1.5 channels that may be associated with inactivation.

Materials and Methods

Molecular biology

The vector pEXO was used to express Kv1.5 and *Shaker* Δ6-46 channels in *Xenopus laevis* oocytes. Cysteine residues were introduced at specific sites (M394C to V401C in Kv1.5, A359C in *Shaker*) in the S3-S4 linker for TMRM-labelling and the only externally accessible cysteine residue, found in the S1-S2 linker, was replaced with a valine residue (C268V in Kv1.5, C245V in *Shaker*) to prevent non-specific dye labelling. The deletion mutation Δ6-46 was introduced into *Shaker* channels to remove fast inactivation [11]. The W472F mutation (equivalent to W434F in *Shaker* channels) was introduced to permanently inactivate channels [12, 13]. To dissociate voltage sensor movement from channel opening, the ILT triple mutation (V407I, I410L and S414T) was introduced in the S4 domain [14, 15]. The H463G mutation in the pore was introduced to enhance inactivation [16]. Point mutations were generated using the Stratagene Quikchange kit (Stratagene, La Jolla, CA) using primers synthesized by SigmaGenosys (Oakville, Ontario), and were sequenced at the University of British Columbia core facility. cRNA was synthesized using the mMessage mMachine T7 Ultra transcription kit (Ambion, Austin, TX) from linearized (*Sac II*) cDNA template.

Solutions and Chemicals

Anaesthetic solution contained 2 g/L of tricaine methane sulphonate, 10 mM HEPES and titrated to pH 7.4 with NaOH. Calcium free solution contained 96 mM NaCl, 3 mM KCl, 1 mM $MgCl_2$, 5 mM HEPES and was titrated to pH 7.4 with NaOH. Barth Solution contains 88 mM NaCl, 1 mM, KCl, 2.4 mM $NaHCO_3$, 0.84 mM $MgSO_4$,

0.41 mM $Ca(NO_3)_2$, 20 mM HEPES and was titrated to pH 7.4 with NaOH. Tetramethylrhodamine (TMRM) labelling of oocytes was performed in a depolarization solution that contained 100 mM KCl, 1.5 mM $MgCl_2$, 0.5 mM $CaCl_2$, 10 mM HEPES and was titrated to pH 7.4 with KOH and 5 μM TMRM. ND96 bath solution contained 1 mM $MgCl_2$, 0.5 mM $CaCl_2$, 5 mM HEPES and either 0.3, 1, 3, 10, 30 or 99 mM KCl with variable concentrations of NaCl so the final concentration of KCl and NaCl was equal to 99 mM. ND96 was either titrated with KOH or NaOH to pH 7.4. Working concentrations of 4-AP were diluted from a 100 mM stock solution made with ND96 solution and was titrated to pH 7.4 using NaOH. TMRM was purchased from Invitrogen (Carlsbad, CA). All other chemicals were purchased from Sigma-Aldrich (Mississauga, ON, Canada).

Oocyte Preparation and Injection

Xenopus laevis were terminally anesthetized in the anesthetic solution described above and the oocytes were removed and placed in Ca^+ free solution. The oocytes were divided into approximate groups of 10 in Ca^+ free solution containing 1 mg/ml of collagenase for 1 hour. This solution was placed on circular rotation at 75 rpm for 1 hour. The oocytes were taken off the rotator when individual oocytes appeared. Oocytes were washed with calcium free solution to remove residual traces of collagenase and stage V-VI oocytes were isolated by manual defolliculation. Isolated oocytes were placed into Ca^+ free solution for at least 30 minutes before injection. After defolliculation, injection electrodes were broken (Drummond Scientific Company, 3-000-210-G8 and pulled to the appropriate shape with Sutter Instruments Model P-97 Glass Puller) and filled with mineral oil from Sigma Aldrich. RNA was aspirated into the

injection pipette and then each oocyte was injected. Oocytes were injected into their animal pole with 50 nl (5-10 ng) of cRNA using a Drummond digital microdispenser (Fisher Scientific, ON, Canada) and then incubated in Barth's solution at 19°C. Currents and fluorescence were recorded 1 to 7 days after injection.

Two electrode voltage clamp fluorometry

Labelling of introduced cysteine residues was performed with TMRM which reacts specifically with cysteine residues and has a maximal light absorption at 542 nm and a maximal emission at 567 nm. 5 µl of TMRM dye was placed into 10 mL of depolarization solutiom (for a final concentration of 5 µM) and oocytes were placed in this solution for 30 minutes at 10°C in the dark. Oocytes were placed in ND96 solution in the dark until they were voltage clamped at room temperature. Fluorometry was performed using a Nikon TE300 inverted microscope with Epi Fluorescence attachment and a 9124b Electron Tubes photomultiplier tube (PMT) module (Cairn Research, Kent, UK). The TMRM dye was excited by light from a 100 Watt mercury arc lamp that was filtered with 525 nm bandpath excitation filter and passed via a dichroic mirror and 20X objective to the oocyte in the bath chamber (Figure 3.1). The fluorescence emission from the dye was collected with the same 20X objective and filtered through a 565 nm long-pass emission filter before being passed to the PMT recording module. Signals from the PMT were digitized using an Axon Digidata 1322 A/D converter and passed to a computer running pClamp8 software (Axon Instruments, Foster City, CA) to record voltage dependent fluorescence emission intensity. Fluorescence signals were unfiltered and recorded with a sampling frequency of 25 kHz. Traces are the average of five sweeps. Voltage clamp of the oocyte and acquisition of the current and voltage clamp

were concurrently attained using the two microelectrode voltage clamp technique with a Warner Instruments OC-725C amplifier (Hamden, CT) Axon Digidata 1322, and pClamp8 software. Glass used as microelectrodes was Glass Thin Wall 1.2 mM diameter and was purchased from World Precision Instruments (Sarasota, Florida). Microelectrodes were filled with 3 M KCl and had a resistance of 0.5 to 1.5 MΩ. Pulled electrodes had a resistance of 0.5 to 1.5 MΩ when placed in ND96 solution.

Data Analysis

Conductance-voltage relation (G-V) curves derived were prepared using the chord conductance that was determined by dividing the maximal current during a depolarization pulse by the driving force derived from the K+ equilibrium potential in which internal K+ was assumed to be 98 mM. G-V curves were fit with a single Boltzmann function:

$$Y = 1/1(1 + \exp(V_{1/2}-V)/k))$$

Where y is the conductance normalized with respect to the maximal conductance, $V_{1/2}$ is the half-activation potential. V is the test voltage and *k* is the slope factor.

F-V relationships were also fit with Boltzmann functions with fluorescence normalized with respect to maximal fluorescence. For the analysis of Kv1.5 M394C and A397C fluorescence, peak minus end analysis was employed to understand the properties of the rapidly decaying phase of the fluorescence signal. The end is defined as ~20 ms after the peak of the fluorescence signal at which point the fluorescence has decayed to a minimum (Fig. 3A). The fluorescence signal at the beginning of the pulse was subtracted from the signal at the minimum and this was divided by the amplitude of the entire

fluorescence signal. This allowed a determination of the percentage of decaying component as a proportion of the total fluorescence signal.

Results

The fluorescence report of voltage sensor movement in Kv1.5 channels is unique

The unique fluorescence report of voltage sensor movement in Kv1.5 channels is demonstrated in Fig. 3.1. For a comparison, the fluorescence report from TMRM attached in the S3-S4 linker at A359C in *Shaker* (Δ6-46) channels is shown in Fig. 3.1A-C. Simultaneous recordings of ionic current (Fig. 3.1A) and TMRM fluorescence (Fig. 3.1B) show that the fluorophore in *Shaker* reports a mono-exponential change in its environment upon depolarization (τ = 2.4 ± 0.5 ms at +60 mV) that occurs with a time course that is similar to the activation of ionic current (τ = 4.5 ± 1.0 ms at +60 mV; n=4). The reported conformational changes display a voltage dependence ($V_{½}$ = -40.9 ± 1.9 mV) that is left-shifted from the G-V relation ($V_{½}$ = -16.2 ± 1.3 mV; Fig. 3.1C), as is expected for movement of the voltage sensors in advance of channel opening. Similar mono-exponential reports of voltage sensor movement that follow at least one component of ionic current activation kinetics have also been reported for hERG, eag, and BK_{Ca} channels [3-5].

In Fig. 3.1D-F, we show, for the first time, the fluorescence report of voltage sensor movement in a mammalian Kv1 channel, Kv1.5. The fluorescence report is from TMRM attached at A397C (the equivalent position in the S3-S4 linker to A359C (Fig. 3.1A-C) in *Shaker* channels). In contrast to the mono-exponential time course of the fluorescence report from *Shaker* (Fig. 3.1B) and other Kv channels [3-5], TMRM attached at Kv1.5 A397C reported a unique and complex profile of fluorescence change (Fig. 3.1E). There were no voltage-dependent fluorescence changes from oocytes expressing Kv1.5 channels that lack an external cysteine residue, and the unusual kinetics of fluorescence change observed in Fig. 3.1E cannot be explained by inadequate voltage

control. Upon depolarization, the fluorescence deflection from Kv1.5 A397C was rapid and transient with a prominent decaying component (τ = 3.4 ± 0.6 ms at +60 mV; n=4) that increased in amplitude with voltage such that it represented 36 ± 3 % of the total signal at +60 mV (the voltage-dependence is described in Figure 3.3). Unlike in *Shaker* A359C (Fig. 3.1C), the F-V relation from Kv1.5 A397C ($V_{½}$ = 1.9 ± 1.9 mV) was not significantly left-shifted from the G-V relation ($V_{½}$ = 7.3 ± 1.6 mV; Fig. 3.1F), and a plot of the voltage dependence of the decaying component of the fluorescence was actually right-shifted ($V_{½}$ = 31.0 ± 2.4 mV) from the G-V relation (Fig. 3.1F). These observations suggest that at least some component of the fluorescence deflection from TMRM attached at Kv1.5 A397C may be coupled in some way with channel opening.

Sites facing the pore report the decaying component of fluorescence

The different report of fluorophore environmental change observed in Kv1.5 (Fig. 3.1D-F) may suggest different voltage sensor conformational changes than in *Shaker* channels. However, a fluorescence scan of the S3-S4 linker of Kv1.5 (Fig. 3.2) reveals that the complex signal is only reported by TMRM at two sites, A397C and M394C (see Fig. 3.3 for a kinetic analysis of Kv1.5 M394C fluorescence). Other sites in the scan do not report the rapid decaying component of fluorescence and produce deflections that are, in general, similar to those described from the equivalent sites in *Shaker* channels [8]. This suggests that Kv1.5 voltage sensor movement *per se* is not dissimilar to that of *Shaker* channels. Instead, since the C-terminal end of the S3-S4 linker likely adopts an α-helical structure [17-19], placing M394C and A397C on the same side of the helix that comes close to the pore domain upon depolarization [8, 20], we hypothesized that TMRM attached at M394C or A397C might be reporting on an additional structural

rearrangement that is associated with opening of the pore. As mentioned, sites S395C, L396C, L399C and V401C all report fluorescence deflections that are similar to those described from similar sites in *Shaker* channels [8]. Interestingly, sites S395C, L396C and L399C that do not report on the rapidly decaying phase found in M394C and A397C have fluorescence-voltage (F-V) relationships that are left shifted from the G-V curves suggesting that the decaying component of fluorescence is a report on channel opening. Furthermore, sites I398C and R400C do not report any voltage dependent fluorescence deflections, despite the analogous residues in *Shaker* providing robust fluorescence signals. I398C provides robust ionic current although there is an absence of any fluorescence report. Interestingly, the mutation of R400 to cysteine did not express as we were unable to record either ionic or fluorescence records. We attempted to adjust R400C expression by holding the oocytes at 12 °C until 6 hours prior to experimentation in order to prevent channel expression to the oocyte membrane to prevent membrane destabilization due to leak current. We then placed the oocytes at 20 °C for 6 hours; however this method failed, as well, to allow us to record either ionic or fluorescence records, suggesting that the lack of R400C expression was due to a trafficking mechanism.

The decaying component of fluorescence reports on an extremely quick rearrangement associated with channel opening

To attempt to understand the decaying component of fluorescence, we quantitated the process. Fitting the decaying component of M394C and A397C fluorescence with a single exponential we found that the decaying component is voltage dependent as it accelerates with greater depolarizations (Fig. 3.3A). Both M394C and A397C report

similar voltage dependence with the sites reporting a time constant of decay of 2.2 ± 0.1 ms and 3.4 ± 0.6 ms, respectively at +60 mV. The extremely quick time constant suggests that the decaying process occurs on a similar time scale as gating and may be therefore associated with channel opening.

To further characterize the decaying component of fluorescence we examined the amount of decay that occurs during a depolarizing pulse (Fig. 3.3B). To determine the percentage of decay we determined the amount of decay 20 ms after the peak of the decaying phase and divided it by the peak signal at the beginning of the pulse. The amount of fluorescence decay was voltage dependent as we recorded larger relaxations of the fluorescence signals with greater depolarizations. Both M394C and A397C report a similar percent of fluorescence decay with a value of decay of 42 ± 4% and 36 ± 3%, respectively. The records from Fig. 3.3 also show the voltage dependence of the measured parameters begin to saturate at greater depolarized potentials. Interestingly, this voltage dependence is extremely similar to that of the opening probability (Fig. 3.1F), and as the opening probability increases to a maximum so does the saturation of the decaying kinetics. This implies that as a greater proportion of channels transition to opening, a greater proportion report on the fast decaying process implying that this process is associated with channel opening.

Noting that this decaying process occurred with an extremely rapid time constant, we attempted to determine the period of time it took the channel to recover in order to report on the decaying process again. To do this we applied a double pulse protocol that began with a 1 s prepulse and then a second pulse was applied at several time points after the first pulse (Fig. 3.4). We found that the decaying process returned with a time

constant of 42 ± 7 ms (Fig. 3.4B). The quick return of the fluorescence report of this process suggests the channel recovers from this conformational rearrangement extremely rapidly.

The decaying component of fluorescence is dependent upon channel opening

To test whether the decaying component of the fluorescence report from Kv1.5 A397C (and M394C) is associated with pore opening, we measured the fluorescence report in the presence of 10 mM 4-aminopyridine (4-AP) or the ILT triple mutation (V407I, I410L, S414T), both of which dissociate voltage sensor movement from channel opening by stabilizing channels in pre-open closed states [14, 15, 21-23].

Prevention of channel opening by the application of 10 mM 4-AP abolished the decaying component of fluorescence (Fig. 3.5A) and reverted the fluorescence phenotype to resemble that reported by *Shaker* A359C (compare the fluorescence trace in the presence of 4-AP with that in Fig. 3.1B). In addition, 4-AP restored the left-shifted voltage dependence of the F-V relation (the $V_{½}$ of the F-V was ~41 mV left-shifted from that of the G-V; Fig. 3.5B). In a similar manner, at potentials (e.g. +60 mV) that stabilize ILT mutant channels in the activated-not-open state [23], the decaying component of fluorescence from Kv1.5 ILT A397C channels was abolished and the *Shaker*-like mono-exponential report of voltage sensor movement was rescued (Fig. 3.5C). The F-V relation in ILT mutant channels was also left-shifted from the G-V relation (the $V_{½}$ of the F-V was –41.6 ± 1.8 mV; Fig. 3.5D). These results demonstrate that the decaying component of fluorescence from A397C is associated in some way with channel opening. Furthermore, the depolarized position of the F-V relation in Fig. 3.1F does not reflect the

true voltage dependence of voltage sensor movement, because it is influenced by an event that TMRM detects upon channel opening.

The decaying component of fluorescence is associated with channel inactivation

Although 4-AP prevents channel opening, drug binding also prevents channel inactivation [24, 25], and it is difficult to assess whether ILT channels inactivate at the strongly depolarized potentials (>+150 mV) required to drive channels into the open state. Therefore, the decaying component of fluorescence may reflect an inactivation process that occurs upon channel opening. To test this, we investigated the effect of manipulations of inactivation on the decaying component of the fluorescence signal (Fig. 3.6).

One of the hallmarks of P/C-type inactivation of Kv channels is its sensitivity to the external K^+ concentration [26]. The fluorescence signals in Fig. 3.6A show that raising the external K^+ concentration to 99 mM abolished the decaying component and restored the *Shaker*-like fluorescence report of voltage sensor movement. With the reduction of inactivation with 99 mM K^+, the F-V relation of voltage sensor movement ($V_{½}$ = -36.4 ± 1.2 mV) becomes apparent (Fig. 3.6B; n=3). In addition, in the presence of the W472F mutation (equivalent to *Shaker* W434F), which stabilizes channels in permanently inactivated states [12, 13], the fluorescence from A397C also shows no rapid decaying component (Fig. 3.6C). The H463G mutation also abolishes current when there is 0 mM K^+(o) through an enhancement of inactivation [16]. The fluorescence from A397C in the presence of H463G mutant also shows no rapid decaying component (Fig. 3.6D). Taken together, these data strongly suggest that the decaying component of

fluorescence reported by TMRM attached at Kv1.5 A397C reflects a process associated with an inactivation transition.

The secondary phase of fluorescence from S395C is associated with channel inactivation

The majority of the focus of this study has been the examination of the decaying phase of fluorescence from sites M394C and A397C. Interestingly, the fluorescence report from site S395C is monoexponential and has characteristics that are similar to the fluorescence from *Shaker* A359C (Figure 3.1C), although the report is inverted. There is an initial fast phase and a secondary slow phase that has been suggested to be associated with voltage sensor movement and inactivation, respectively [9]. In this initial study of Kv1.5 fluorescence we attempted to understand the fluorescence from site S395C by modification of the channel with 10 mM 4-AP and raising extracellular K^+ from 3 mM to 99 mM. We found that both conditions reduced the fast phase of fluorescence and completely abolished the slow secondary phase (Figures 3.7A and B). As well as the loss of secondary fluorescence by blocking the channel with 10 mM 4-AP (Figure 3.7A) the fluorescence report from S395C shows a robust transient off fluorescence. This report hints that the voltage sensor instantaneously returns to a position similar to that of the control before returning to its resting state. Although only preliminary, this data suggests that the slow secondary phase of fluorescence from site S395C may report on inactivation and could possibly be used in future studies to examine voltage sensor movement and inactivation in Kv1.5.

Discussion

In this description of the first fluorescence reports of the conformational rearrangements associated with gating of a mammalian Kv1 channel, we observed complex fluorescence changes in the report of voltage sensor movements in Kv1.5 channels (Fig. 3.1). This complex report of environmental changes occurring around the fluorophore attached at A397C (and M394C) upon depolarization (Figs. 3.1 and 3.2) suggests unique and complex motions of the voltage sensor domains in Kv1.5 channels that are quite different from those reported in *Shaker* channels [1, 2]. However, we do not believe that this is the case because: 1) only sites that face the pore domain (A397C and M394C) report the complex changes; 2) many of the sites that do not report the rapid inactivation process have F-V relations that are well left-shifted from the G-V relations (the $V_{½}$ values for the F-V relations of S395C, L396C and L399C were 64, 12, and 48 mV left-shifted from the corresponding $V_{½}$ values for the G-V relations) as would be predicted for a faithful report of *Shaker*-like voltage sensor movement; 3) prevention of channel opening by 4-AP or the ILT triple mutation (Fig. 3.5), or of inactivation by raising external K^+ (Fig. 3.6), unmasks the kinetics and voltage dependence of voltage sensor movement by abolishing the decaying component of fluorescence. Instead, we believe that the fluorescence report from M394C and A397C is complex because it reflects a composite of conformational rearrangements associated not only with activation of the voltage sensors, but also with a rapid structural reorganization that is associated with the pore domain of the channel upon opening. This conclusion is consistent with electrophysiological and crystallographic data, which demonstrate that each voltage sensor comes into close proximity with the outer pore S5-P linker of its adjacent subunit upon depolarization [7, 8, 17, 20, 27-32], and is supported by previous

observations of structural changes reported by sites within the S3-S4 linker that are associated with opening of the intracellular gate and/or inactivation of the outer pore [3, 5, 7-9, 21, 25, 33].

The observations that the rapidly decaying component of fluorescence was abolished by manipulations that inhibit inactivation [34], such as raising external K^+ (Fig. 3.6A), suggest that the structural changes associated with pore opening reported by TMRM at A397C and M394C in Kv1.5 are coupled with a rapid inactivation related process. P/C-type inactivation is a common feature of Kv channel gating and involves constriction of the outer pore and a reduction in channel availability [35-37]. P/C-type inactivation is known to occur in Kv1.5 channels [38] and is observed as a slow decline of current during sustained (hundreds of ms to s) depolarization or a reduction in peak current during repetitive short depolarizing pulses. Therefore the process that we describe which occurs with a time constant of several milliseconds may be a previously uncharacterized rapid component of inactivation or a preliminary process that leads to inactivation. Further studies are required to distinguish between these possibilities, but given the rapid return of the fluorescence signal to baseline upon repolarization (Fig. 3.1E) and the observation that the fluorescence amplitude recovers fully even with rest intervals as short as 2 s (data shown in Fig. 3.1E are the average of five sweeps applied at 0.5 Hz), channels do not appear to undergo appreciable C-type inactivation during the rapid decay of fluorescence.

Figure 3.1 Characteristics of the TMRM fluorescence report from Kv1.5 A397C channels.

A, B, D and E, representative ionic current (A and D) and fluorescence (B and E) traces recorded from oocytes expressing *Shaker* A359C (A and B) or Kv1.5 A397C (D and E) channels labelled with TMRM. Voltage clamp pulses were applied from -80 to +60 mV in 10 mV increments (100 ms duration) from a holding potential of -80 mV (only highlighted traces are shown for clarity). C and F, mean G-V (●) and F-V (○) relations for *Shaker* A359C (*C*; n=3) and Kv1.5 A397C (*F*; n=4). $V_{1/2}$ and k values for the G-V relation of *Shaker* A359C channels were -16.2 ± 1.3 mV and 16.8 ± 1.1 mV, respectively, and the corresponding values for the F-V relation were -40.9 ± 1.9 mV and 17.0 ± 1.7 mV, respectively. $V_{1/2}$ and k values for the G-V relation of Kv1.5 A397C were 7.3 ± 1.6 mV and 16.4 ± 1.2 mV, respectively, and the corresponding values for the F-V relation were 1.9 ± 1.9 mV and 19.0 ± 1.3 mV, respectively. The F-V relation was not significantly shifted from the G-V relation. The voltage dependence of the decaying component of fluorescence from Kv1.5 A397C (calculated as the peak minus end fluorescence amplitude) is also shown in panel *F* (▼); $V_{1/2}$ and k values were 31.0 ± 2.4 mV and 15.5 ± 1.9 mV, respectively.

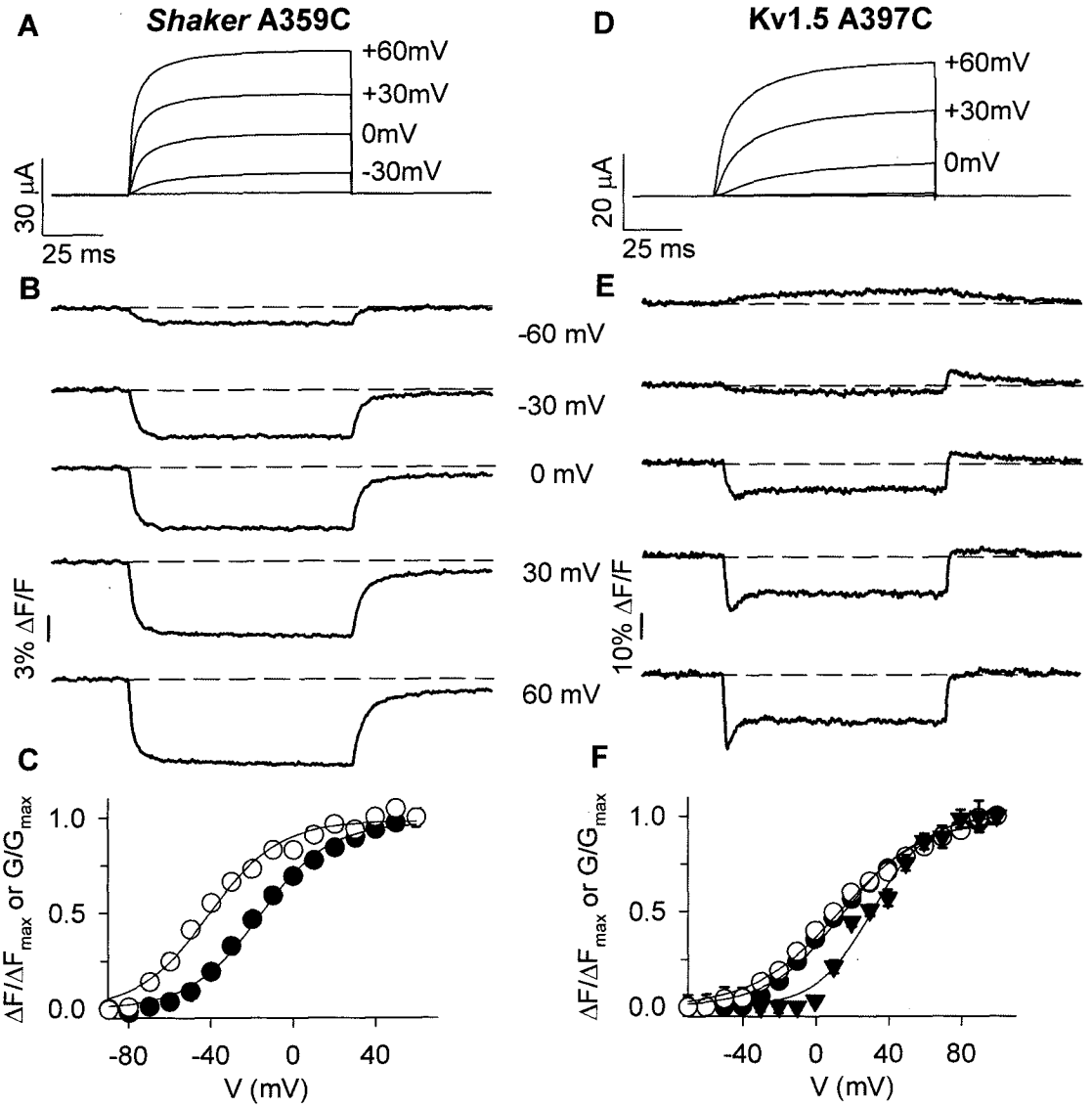
A
Shaker A359C
+60mV
+30mV
0mV
-30mV
30 µA
25 ms
D
Kv1.5 A397C
+60mV
+30mV
0mV
20 µA
25 ms
B
-60 mV
-30 mV
0 mV
30 mV
60 mV
3% ΔF/F
E
10% ΔF/F
C
ΔF/ΔF_max or G/G_max
1.0
0.5
0.0
-80
-40
0
40
V (mV)
F
ΔF/ΔF_max or G/G_max
1.0
0.5
0.0
-40
0
40
80
V (mV)

Figure 3.2 Sites facing the pore report the rapid decaying component of fluorescence.
Representative fluorescence signals recorded from TMRM attached at each site in the Kv1.5 S3-S4 linker from M394C to V401C during 100 ms voltage clamp pulses from -80 to +60 mV. Scale bars represent a 1 % ΔF/F fluorescence deflection. Mean G-V (●) and F-V (○) relations for each mutation, alongside the associated fluorescence deflection. Boltzmann fits of the data gave $V_{½}$ and k values for G-V and F-V relations of: 6.9 ± 1.9 and 17.3 ± 1.4 mV (G-V), respectively, and -10.5 ± 1.9 and 19.4 ± 1.4 mV (F-V), respectively, for M394C (n=4); 9.0 ± 1.4 and 17.2 ± 1.0 mV (G-V), respectively, and –54.7 ± 0.8 and 9.7 ± 0.7 mV (F-V), respectively, for S395C (n=7); -19.7 ± 1.8 and 16.2 ± 1.5 mV (G-V), respectively, and –31.5 ± 3.3 and 25.1 ± 2.8 mV (F-V), respectively, for L396C (n=3); 7.4 ± 1.6 and 16.4 ± 1.2 mV (G-V), respectively, and 2.0 ± 1.9 and 18.9 ± 1.3 mV (F-V), respectively, for A397C (n=4); -18.1 ± 3.4 and 21.6 ± 2.7 mV (G-V), respectively, and –66.4 ± 1.6 and 7.2 ± 1.5 mV (F-V), respectively, for L399C (n=3); 10.8 ± 1.2 and 13.3 ± 0.9 mV (G-V), respectively, and 25.7 ± 2.2 and 23.3 ± 1.0 mV (F-V), respectively, for V401C (n=7); voltage-dependent fluorescence deflections were not evident with TMRM attached at I398C, and R400C channels did not express ionic current. The voltage dependence of the decaying component of fluorescence (calculated as the peak minus end fluorescence amplitude) is also shown (▼) for M394C and A397C. In the case of M394C, $V_{½}$ and k values were 5.8 ± 1.8 and 10.9 ± 1.5 mV (n=4), respectively, and the corresponding values for A397C were 40.0 ± 6.8 and 16.2 ± 2.9 mV (n=4).

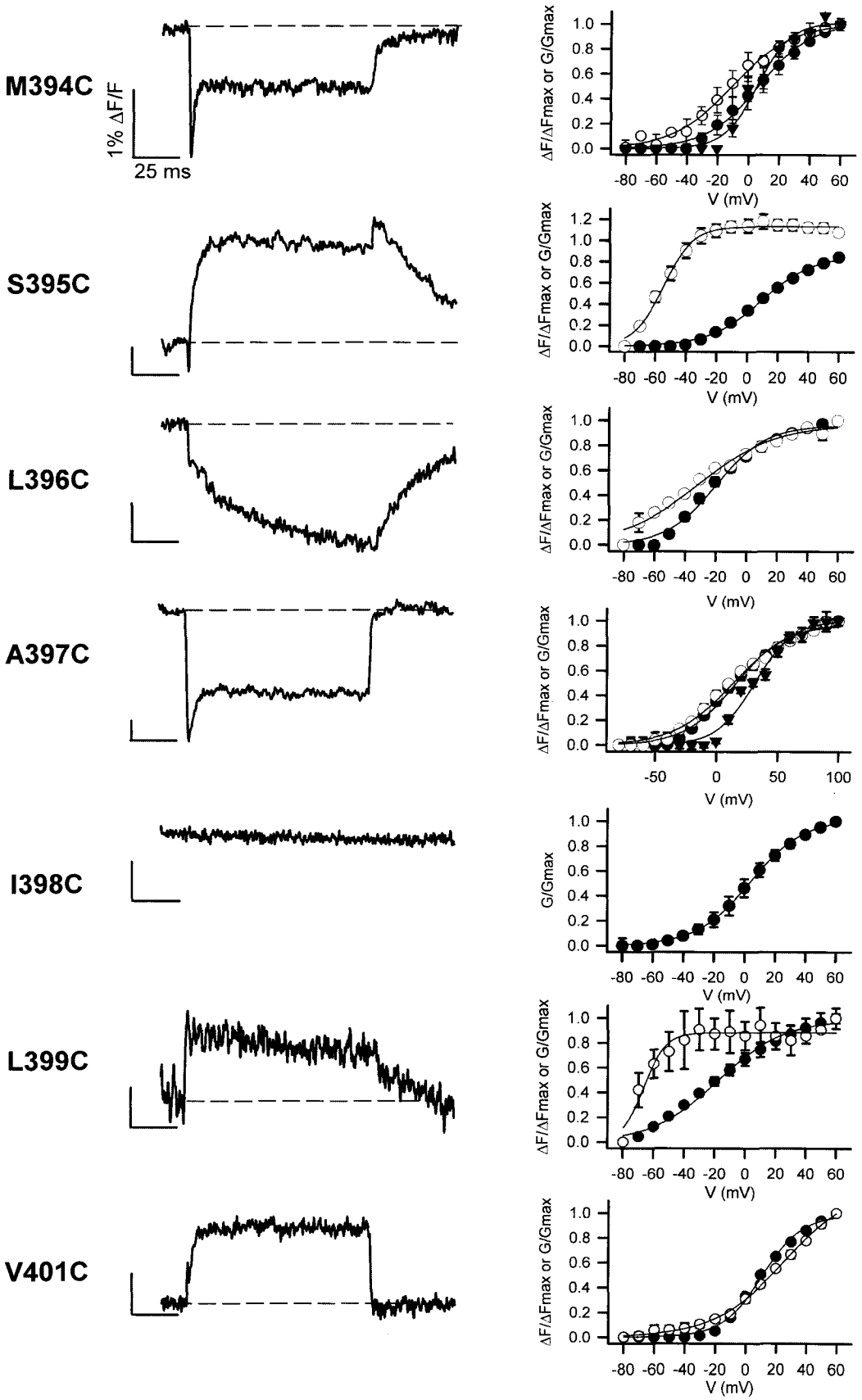
M394C
1% ΔF/F
25 ms
S395C
L396C
A397C
I398C
L399C
V401C
ΔF/ΔFmax or G/Gmax
G/Gmax
V (mV)

Figure 3.3 Characterization of the decaying component of fluorescence.

A, fitting the decaying phase of fluorescence of M394C and A397C with a single exponential function shows that the time constant of the decaying phase decreases to a maximum at +60 mV of 2.2 ± 0.1 ms and 3.4 ± 0.6 ms for M394C and A397C, respectively. B, determining the percent fluorescence decay of M394C and A397C, by peak minus end analysis, shows that the decaying phase increases as a percentage of the total fluorescence signal to a maximum at +60 mV of 42 ± 4% and 36 ± 3% for M394C and A397C, respectively (n=5).

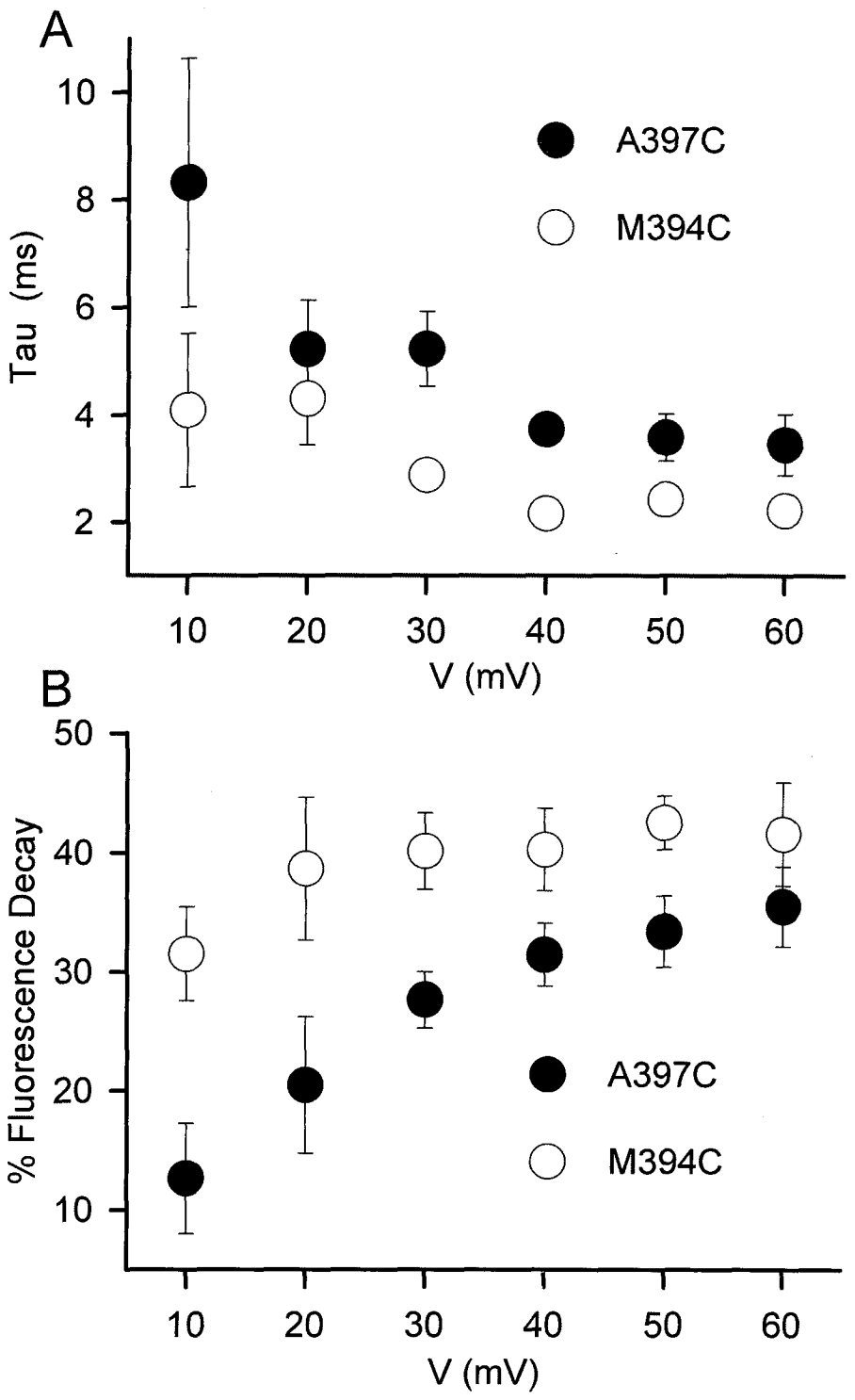
A
10
8
6
4
2
Tau (ms)
A397C
M394C
10
20
30
40
50
60
V (mV)
B
50
40
30
20
10
% Fluorescence Decay
A397C
M394C
10
20
30
40
50
60
V (mV)

Figure 3.4 Recovery of decaying phase after a prepulse.

A, representative fluorescence signals recorded from TMRM attached at site A397C in the Kv1.5 S3-S4 linker after applying a 1 second prepulse to +60 mV from a holding potential of -80 mV. B, application of a second pulse to +60 mV at 0.015, 0.035, 0.075, 0.12, 0.15, 0.3 and 0.9 seconds after the 1 second prepulse resulted in the decaying component of fluorescence to return with a time constant of 42 ± 7 milliseconds (n=5).

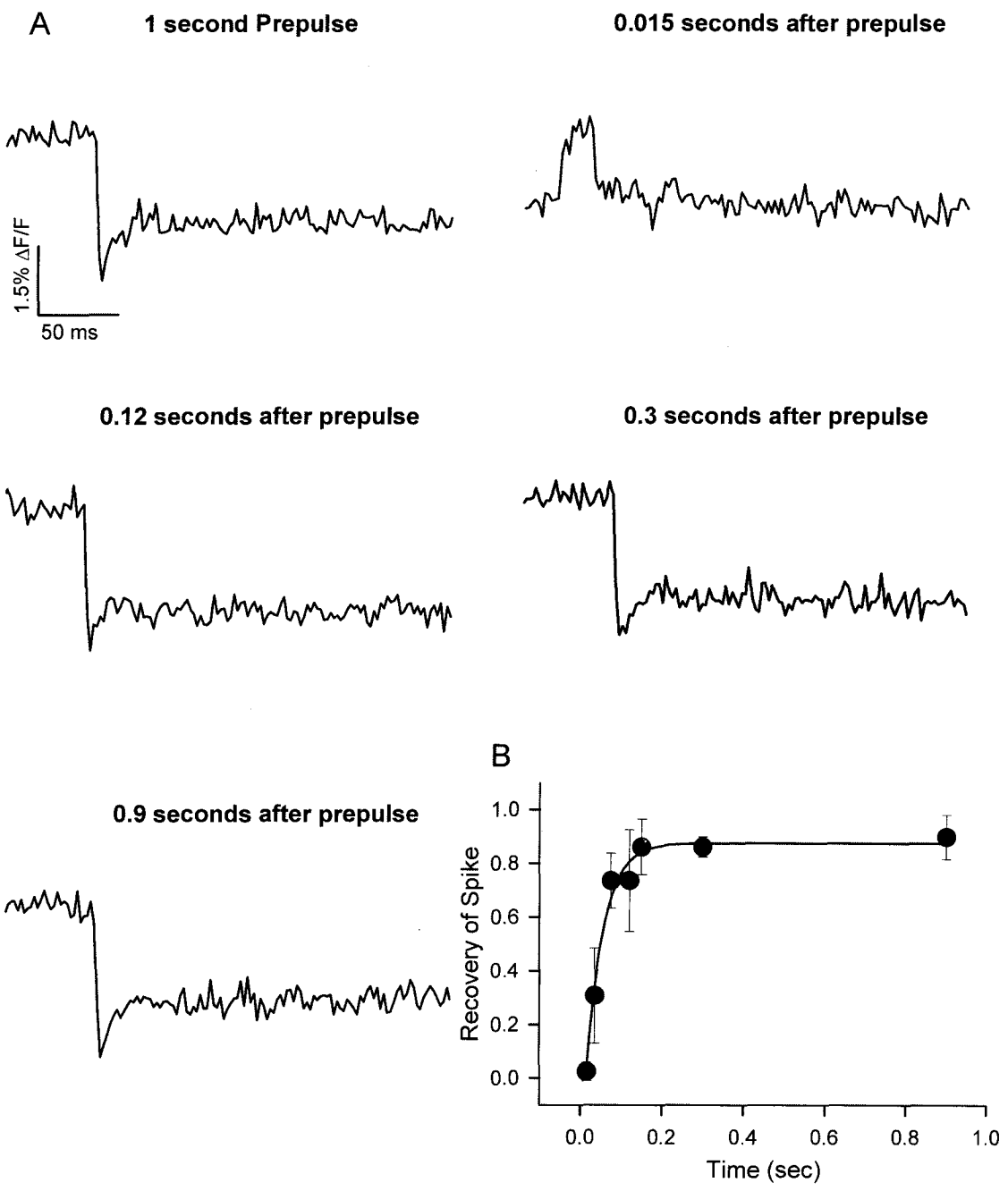
A
1 second Prepulse
0.015 seconds after prepulse
1.5% ΔF/F
50 ms
0.12 seconds after prepulse
0.3 seconds after prepulse
0.9 seconds after prepulse
B
Recovery of Spike
1.0
0.8
0.6
0.4
0.2
0.0
0.0
0.2
0.4
0.6
0.8
1.0
Time (sec)

Figure 3.5 The decaying component of fluorescence is associated with channel opening.
A, representative fluorescence signals recorded from TMRM attached at A397C during control conditions and in the presence of 10 mM 4-AP during 100 ms voltage clamp pulses from -80 to +60 mV. Block with 10 mM 4-AP prevented channel opening and reduced current amplitude by 66 ± 6 % (n=3). B, mean G-V and F-V relations in the presence of 10 mM 4-AP. $V_{½}$ and k values for G-V and F-V relations were 44.0 ± 2.8 and 23.6 ± 1.7 mV (G-V), and 3.2 ± 2.5 and 18.8 ± 2.1 mV (F-V; n=3). The F-V relation was therefore 41 mV left-shifted from the G-V relation. C, representative fluorescence signals recorded from A397C in the presence of the ILT mutation during 100 ms voltage clamp pulses to +60 mV. The ILT mutation uncouples independent voltage sensor movement from the concerted opening transition (15, 16) resulting in a shift of the G-V relation to depolarized potentials (see panel D). D, mean G-V and F-V relations for Kv1.5 A397C ILT channels. $V_{½}$ and k values for G-V and F-V relations were 131.0 ± 1.2 and 21.4 ± 0.8 mV (G-V), respectively, and –41.6 ± 1.8 and 20.6 ± 1.7 mV (F-V; n=3). The F-V relation was therefore 173 mV left-shifted from the G-V relation.

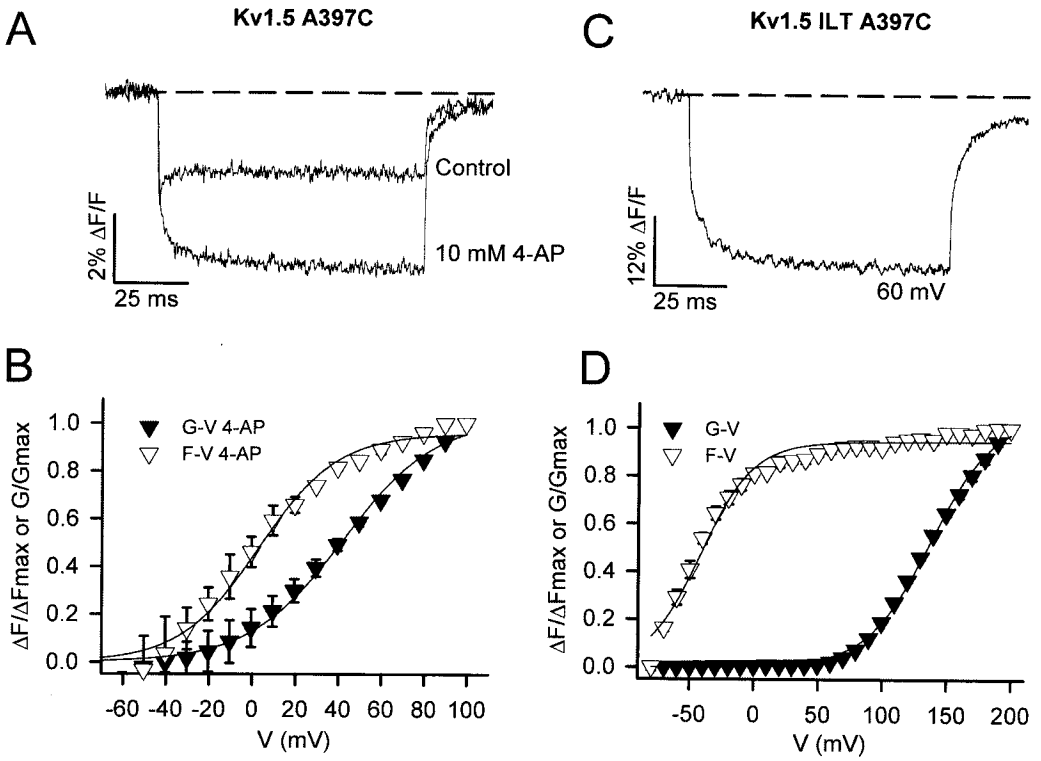
A
Kv1.5 A397C
Control
10 mM 4-AP
2% ΔF/F
25 ms
C
Kv1.5 ILT A397C
12% ΔF/F
25 ms
60 mV
B
G-V 4-AP
F-V 4-AP
ΔF/ΔFmax or G/Gmax
V (mV)
D
G-V
F-V
ΔF/ΔFmax or G/Gmax
V (mV)

Figure 3.6 Manipulation of inactivation alters the decaying component of fluorescence.

A, representative fluorescence signals recorded from Kv1.5 A397C channels during 100 ms pulses to +60 mV in the presence of 3 and 99 mM external K^+. Inhibition of inactivation by raising K^+ abolished the rapid decaying component of fluorescence. B, mean F-V relation with 99 mM K^+ plotted alongside the G-V and F-V relations obtained with 3 mM K^+ to demonstrate the voltage dependence of voltage sensor movement in the absence of inactivation. The G-V relation with 99 mM K^+ is not shown because of the large error associated with calculations around the reversal potential (~0 mV). $V_{½}$ and k values for the F-V relation with 99 mM K^+ were –36.4 ± 1.2 and 12.8 ± 1.0 mV, respectively (n=3). $V_{½}$ and k values for the G-V and F-V relations with 3 mM K^+ were 8.1 ± 2.5 and 18.3 ± 1.7 mV and 4.3 ± 2.0 and 21.5 ± 1.3 mV, respectively (n=3). The F-V relation with high external K^+ was therefore 40 mV left-shifted from the G-V relation. C and D, representative fluorescence signals recorded from Kv1.5 A397C W472F mutant channels (C), which are permanently inactivated, or from Kv1.5 A397C H463G mutant channels at 0 mM external K^+ (D) in which the channel is inactivated, during 100 ms voltage clamp pulses from -80 to +60 mV. Similar recordings were obtained from nine (W472F) or three (H463G) other cells.

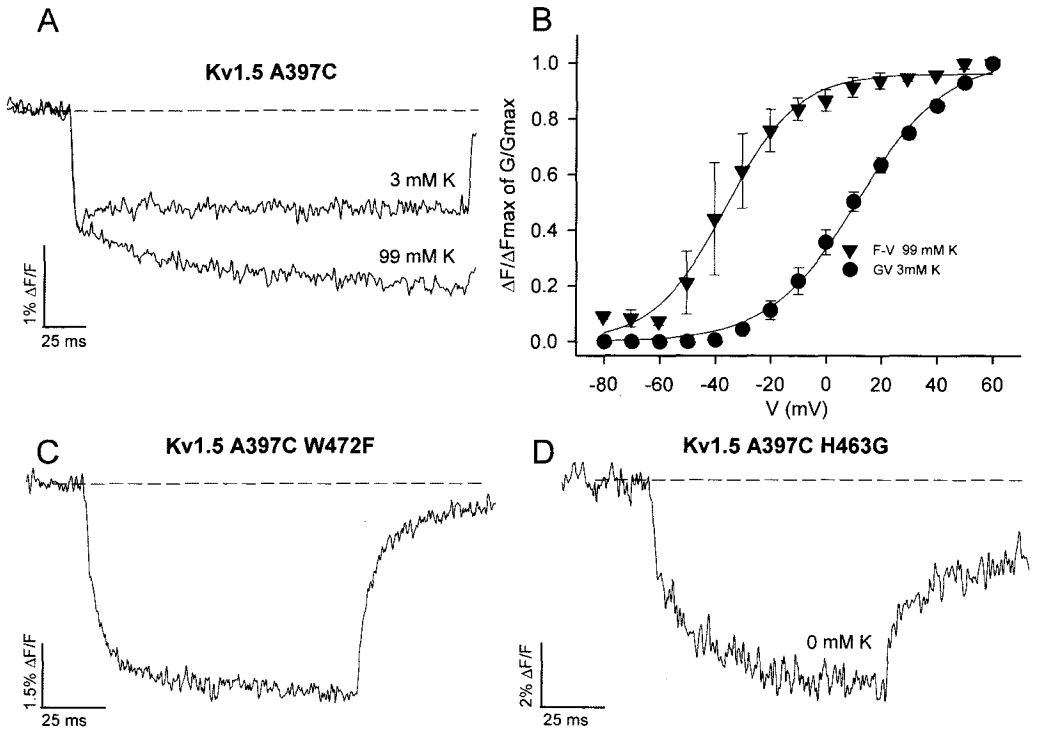
A
Kv1.5 A397C
3 mM K
99 mM K
1% ΔF/F
25 ms
B
1.0
0.8
0.6
0.4
0.2
0.0
ΔF/ΔFmax of G/Gmax
-80
-60
-40
-20
0
20
40
60
V (mV)
F-V 99 mM K
GV 3mM K
C
Kv1.5 A397C W472F
1.5% ΔF/F
25 ms
D
Kv1.5 A397C H463G
0 mM K
2% ΔF/F
25 ms

Figure 3.7 Manipulation of inactivation alters the secondary component of fluorescence from S395C.
A, representative fluorescence signals recorded from TMRM attached at S395C during control conditions and in the presence of 10 mM 4-AP during 200 ms voltage clamp pulses from -80 to +60 mV. Control S395C fluorescence reports a monoexponential fluorescence report with an observable fast phase and a secondary slow phase. 10 mM 4-AP prevented channel opening and reduced fluorescence amplitude as the secondary phase was abolished. B, representative fluorescence signals recorded from TMRM attached at S395C during control conditions at 3 mM K^+ and 99 mM K^+ during 200 ms voltage clamp pulses from -80 to +60 mV. 99 mm K^+ abolished the secondary phase of fluorescence that is observable at 3 mM K^+.

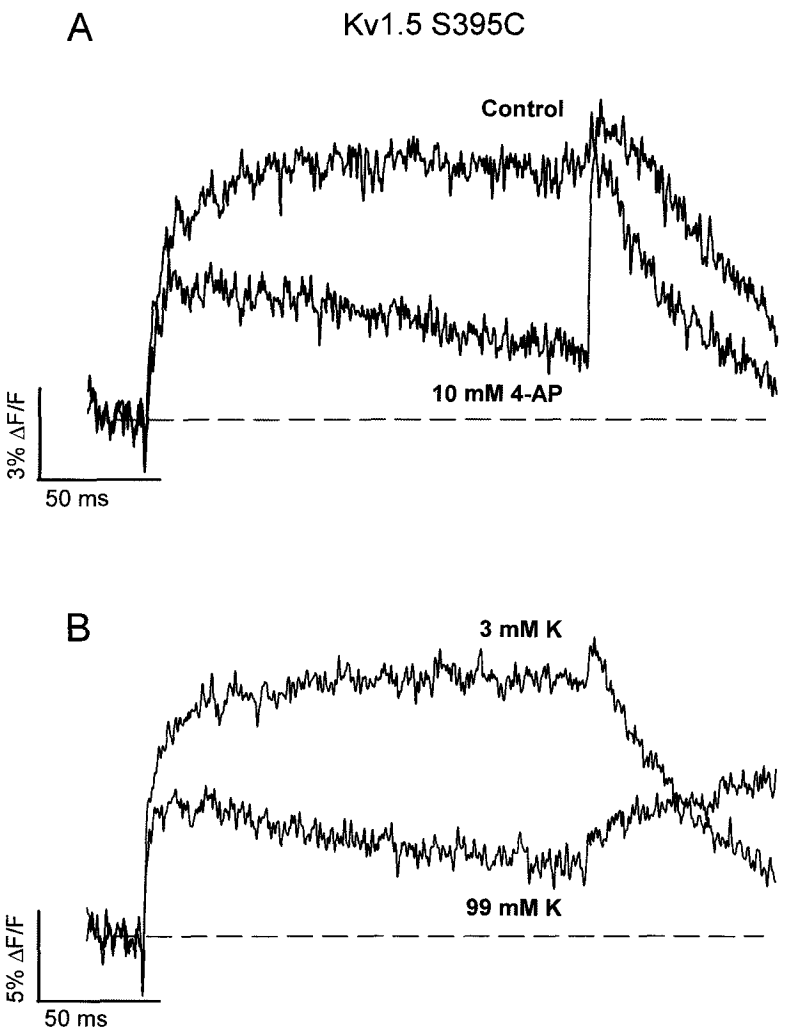
A
Kv1.5 S395C
Control
10 mM 4-AP
3% ΔF/F
50 ms
B
3 mM K
99 mM K
5% ΔF/F
50 ms

References

1. Mannuzzu, L.M., M.M. Moronne, and E.Y. Isacoff, *Direct physical measure of conformational rearrangement underlying potassium channel gating.* Science, 1996. **271**(5246): p. 213-6.
2. Cha, A. and F. Bezanilla, *Characterizing voltage-dependent conformational changes in the Shaker K+ channel with fluorescence.* Neuron, 1997. **19**(5): p. 1127-40.
3. Smith, P.L. and G. Yellen, *Fast and slow voltage sensor movements in HERG potassium channels.* J Gen Physiol, 2002. **119**(3): p. 275-93.
4. Bannister, J.P., et al., *Optical detection of rate-determining ion-modulated conformational changes of the ether-a-go-go K+ channel voltage sensor.* Proc Natl Acad Sci U S A, 2005. **102**(51): p. 18718-23.
5. Savalli, N., et al., *Voltage-dependent conformational changes in human Ca(2+)- and voltage-activated K(+) channel, revealed by voltage-clamp fluorometry.* Proc Natl Acad Sci U S A, 2006. **103**(33): p. 12619-24.
6. Savalli, N., et al., *Modes of operation of the BKCa channel beta2 subunit.* J Gen Physiol, 2007. **130**(1): p. 117-31.
7. Loots, E. and E.Y. Isacoff, *Molecular coupling of S4 to a K(+) channel's slow inactivation gate.* J Gen Physiol, 2000. **116**(5): p. 623-36.
8. Gandhi, C.S., E. Loots, and E.Y. Isacoff, *Reconstructing voltage sensor-pore interaction from a fluorescence scan of a voltage-gated K+ channel.* Neuron, 2000. **27**(3): p. 585-95.

9. Loots, E. and E.Y. Isacoff, *Protein rearrangements underlying slow inactivation of the Shaker K+ channel.* J Gen Physiol, 1998. **112**(4): p. 377-89.

10. Piper, D.R., et al., *Gating currents associated with intramembrane charge displacement in HERG potassium channels.* Proc Natl Acad Sci U S A, 2003. **100**(18): p. 10534-9.

11. Hoshi, T., W.N. Zagotta, and R.W. Aldrich, *Biophysical and molecular mechanisms of Shaker potassium channel inactivation.* Science, 1990. **250**(4980): p. 533-8.

12. Perozo, E., et al., *Gating currents from a nonconducting mutant reveal open-closed conformations in Shaker K+ channels.* Neuron, 1993. **11**(2): p. 353-8.

13. Yang, Y., Y. Yan, and F.J. Sigworth, *How does the W434F mutation block current in Shaker potassium channels?* J Gen Physiol, 1997. **109**(6): p. 779-89.

14. Smith-Maxwell, C.J., J.L. Ledwell, and R.W. Aldrich, *Uncharged S4 residues and cooperativity in voltage-dependent potassium channel activation.* J Gen Physiol, 1998. **111**(3): p. 421-39.

15. Smith-Maxwell, C.J., J.L. Ledwell, and R.W. Aldrich, *Role of the S4 in cooperativity of voltage-dependent potassium channel activation.* J Gen Physiol, 1998. **111**(3): p. 399-420.

16. Zhang, S., et al., *Constitutive inactivation of the hKv1.5 mutant channel, H463G, in K+-free solutions at physiological pH.* Cell Biochem Biophys, 2005. **43**(2): p. 221-30.

17. Li-Smerin, Y. and K.J. Swartz, *Helical structure of the COOH terminus of S3 and its contribution to the gating modifier toxin receptor in voltage-gated ion channels.* J Gen Physiol, 2001. **117**(3): p. 205-18.

18. Li-Smerin, Y., D.H. Hackos, and K.J. Swartz, *alpha-helical structural elements within the voltage-sensing domains of a K(+) channel.* J Gen Physiol, 2000. **115**(1): p. 33-50.

19. Gonzalez, C., et al., *Periodic perturbations in Shaker K+ channel gating kinetics by deletions in the S3-S4 linker.* Proc Natl Acad Sci U S A, 2001. **98**(17): p. 9617-23.

20. Elinder, F., R. Mannikko, and H.P. Larsson, *S4 charges move close to residues in the pore domain during activation in a K channel.* J Gen Physiol, 2001. **118**(1): p. 1-10.

21. Pathak, M., et al., *The cooperative voltage sensor motion that gates a potassium channel.* J Gen Physiol, 2005. **125**(1): p. 57-69.

22. McCormack, K., W.J. Joiner, and S.H. Heinemann, *A characterization of the activating structural rearrangements in voltage-dependent Shaker K+ channels.* Neuron, 1994. **12**(2): p. 301-15.

23. del Camino, D., M. Kanevsky, and G. Yellen, *Status of the intracellular gate in the activated-not-open state of shaker K+ channels.* J Gen Physiol, 2005. **126**(5): p. 419-28.

24. Castle, N.A., et al., *4-Aminopyridine binding and slow inactivation are mutually exclusive in rat Kv1.1 and Shaker potassium channels.* Mol Pharmacol, 1994. **46**(6): p. 1175-81.

25. Claydon, T.W., et al., *4-aminopyridine prevents the conformational changes associated with P/C-type inactivation in Shaker channels.* J Pharmacol Exp Ther, 2006.

26. Baukrowitz, T. and G. Yellen, *Modulation of K+ current by frequency and external [K+]: a tale of two inactivation mechanisms.* Neuron, 1995. **15**(4): p. 951-60.

27. Blaustein, R.O., et al., *Tethered blockers as molecular 'tape measures' for a voltage-gated K+ channel.* Nat Struct Biol, 2000. **7**(4): p. 309-11.

28. Laine, M., et al., *Atomic proximity between S4 segment and pore domain in Shaker potassium channels.* Neuron, 2003. **39**(3): p. 467-81.

29. Larsson, H.P. and F. Elinder, *A conserved glutamate is important for slow inactivation in K+ channels.* Neuron, 2000. **27**(3): p. 573-83.

30. Long, S.B., E.B. Campbell, and R. Mackinnon, *Crystal structure of a mammalian voltage-dependent Shaker family K+ channel.* Science, 2005. **309**(5736): p. 897-903.

31. Ortega-Saenz, P., et al., *Collapse of conductance is prevented by a glutamate residue conserved in voltage-dependent K(+) channels.* J Gen Physiol, 2000. **116**(2): p. 181-90.

32. Long, S.B., E.B. Campbell, and R. Mackinnon, *Voltage sensor of Kv1.2: structural basis of electromechanical coupling.* Science, 2005. **309**(5736): p. 903-8.

33. Claydon, T.W., et al., *A direct demonstration of closed-state inactivation of K+ channels at low pH.* J Gen Physiol, 2007. **129**(5): p. 437-55.

34. Lopez-Barneo, J., et al., *Effects of external cations and mutations in the pore region on C-type inactivation of Shaker potassium channels.* Receptors Channels, 1993. **1**(1): p. 61-71.

35. Yellen, G., *Premonitions of ion channel gating.* Nat Struct Biol, 1998. **5**(6): p. 421.

36. Liu, Y., M.E. Jurman, and G. Yellen, *Dynamic rearrangement of the outer mouth of a K+ channel during gating.* Neuron, 1996. **16**(4): p. 859-67.

37. Yellen, G., et al., *An engineered cysteine in the external mouth of a K+ channel allows inactivation to be modulated by metal binding.* Biophys J, 1994. **66**(4): p. 1068-75.

38. Snyders, D.J., M.M. Tamkun, and P.B. Bennett, *A rapidly activating and slowly inactivating potassium channel cloned from human heart. Functional analysis after stable mammalian cell culture expression.* J Gen Physiol, 1993. **101**(4): p. 513-43.

Chapter 4

Final Discussion and Conclusions

The data presented in this thesis provide insight into the technique of voltage clamp fluorometry and how this technique can be used to gain knowledge into the structure and function of voltage-gated ion channels. The work has allowed us to further our understanding of drug block of ion channels and processes related to channel gating and the intricate relationship between the voltage sensor and the outer pore of the channel. Also, the Kv1.5 fluorescence study was the first study of a mammalian Kv1 channel other than the *Shaker* channel.

4-AP project

As mentioned, 4-aminopyridine has been extensively studied and the mechanism of its block was thought to be fully understood [1-4]. The drug had been suggested to bind to the channel and prevent it from entering the inactivated state [1]. However, experiments performed with voltage clamp fluorometry have suggested that 4-AP can bind to the P-type inactivated state of the channel and prevent C-type inactivation from occurring. This is the first comprehensive study of the effect of drug binding on voltage-gated ion channels using voltage clamp fluorometry. It revealed interactions with electrically silent states that are not possible to observe with traditional patch clamp techniques.

Kv1.5 Fluorescence Study

The Kv1.5 data are the first from mammalian Kv1 voltage-gated channels obtained with voltage clamp fluorometry. VCF revealed that although *Shaker* and Kv1.5 channels share a considerable homology in the S4 and pore region, the fluorescence report of Kv1.5 at sites M394C and A397C contrasted with those of the *Shaker* channel at the analogous M356C and A359C sites [5-7]. The fluorescence report from Kv1.5 revealed a prominent decaying phase that was absent in the *Shaker* channel, although the other sites from the Kv1.5 S3-S4 linker showed similar reports to *Shaker* [7]. Modification of channel gating by the ILT triple mutation and 4-AP suggested that this was a report on a rapid process that was associated with channel opening. The mutations W472F and H463G suggested that the process might be an outer pore rearrangement that was prevented when the channel was modified into a permanently P-type inactivated state. This implies that the process observed by voltage clamp fluorometry is associated with inactivation, although more experiments are required to fully understand this process.

Future Directions

The two studies described in this thesis show that VCF is a powerful technique that can be used to further our understanding of ion channel gating. The potential of this recently developed technique is only beginning to be exploited to further our knowledge of the intricacies of ion channel structure. Our work suggests that there are many future experiments to be attempted and several future studies related to the work in this thesis are outlined below.

Channel Modification

The study of 4-AP block is one of the very first studies describing the alteration of ion channel gating by VCF. It is expected that as additional channels are studied with VCF and the fluorescence reports from these channels are characterized, researchers will be able to examine residues that report on conformational rearrangements associated with drug binding and residues involved in drug interactions. This will allow insight into the mechanism and residues that are important in drug block in real time. In addition to studying drug block, researchers have attempted to determine the mechanism of action of auxillary subunits, pH and inactivation on ion channel function [8-10]. These studies have all shown that once fluorescence reports from ion channels have been characterized, they can be used to improve our understanding of controversial issues within the ion channel field.

Kv1.5 Closed State Transitions

The study of Kv1.5 fluorescence revealed a novel electrically silent rearrangement of the outer pore mouth that is associated with channel opening. However, there are interesting fluorescence reports from several sites in the S3-S4 linker of the Kv1.5 channel at hyperpolarized potentials. The sites A397C and L399C reveal large fluorescence deflections that are as large or larger in magnitude than the fluorescence deflections seen at depolarized potentials. This indicates that the voltage sensor may be undergoing large-scale conformational rearrangements at hyperpolarized potentials and these rearrangements may be not associated with channel opening. These

rearrangements may possibly be a pre-open state of the channel. Further experiments are required to elucidate the structural rearrangements that are being reported at hyperpolarized potentials.

Kv1.5 Gating and Inactivation

Another future study that could help to further explain the conformational changes reported by sites M394C and A397C is a complete cysteine scan of the outer pore (S5-P loop-S6) of Kv1.5. We initially examined two sites, G461C and T462C, which are found in the S5-Plinker of the turret of Kv1.5. However, the fluorescence report from G461C was small in magnitude and was difficult to resolve and analyze (Fig. 4.1A) and TMRM attached to site T462C blocked the channel and prevented ion flow, although the associated fluorescence report was robust (Fig. 4.1B). If other sites in the pore are examined they may help to further understand the conformational changes associated with channel opening reported by the S3-S4 linker or other electrically silent transitions. Also, as mentioned, a comprehensive study of the outer pore of Kv1.5 may help to reveal sites that may be useful in drug binding experiments as well as sites that may aid in our understanding of the effect of auxiliary subunits on channel function.

As noted in Chapter 3, the fluorescence reports from other sites in the S3-S4 linker are exponential in nature. In particular, sites S395C and L396C both report an initial fast phase followed by a slow secondary phase. Figures 3.7A and 3.7B show that the secondary phase of the fluorescence from site S395C is abolished by 4-AP and 99 mM K^+, respectively. This implies that this secondary phase may be a report on channel inactivation and therefore may be useful in future studies examining inactivation reported

from the Kv1.5 voltage sensor. However, before such a study can be attempted, variation of pulse duration is required to determine if this secondary phase is indeed associated with channel inactivation, similar to the original studies in *Shaker* [10]. There remain a number of unresolved questions with Kv1.5 fluorescence that may lead to our further understanding of the mechanism of ion channel gating.

Figure 4.1 Fluorescence from sites G461C and T462C do not report on the rapidly decaying phase of fluorescence reported from the S3-S4 linker of Kv1.5.

A, representative fluorescence signals recorded from TMRM attached at G461C during control conditions at 3 mM K^+ during 100 ms voltage clamp pulses from -80 to +60 mV. G461C fluorescence reports a fast fluorescence signal that is small in magnitude and difficult to resolve. B, representative fluorescence signals recorded from TMRM attached at T462C during control conditions at 3 mM K^+ during 100 ms voltage clamp pulses from -80 to +60 mV. The fluorescence reports on an initial fast transient followed by a slow secondary phase. Ionic current (not shown) is abolished when TMRM is attached to the channel at site T462C.

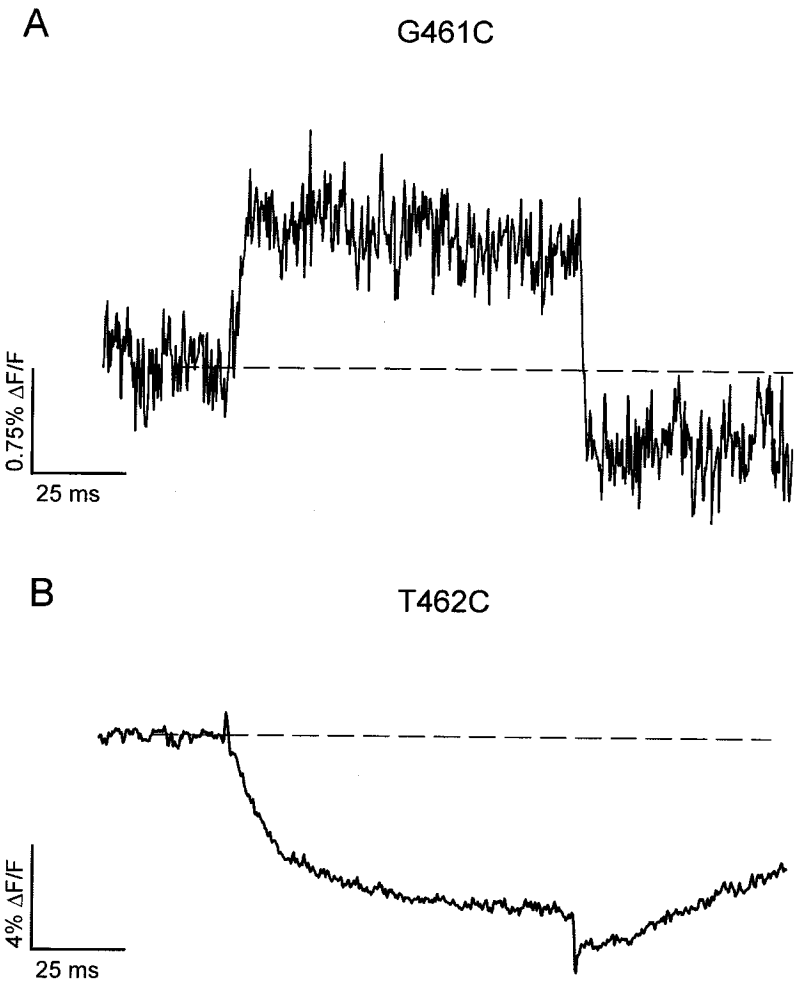
A
G461C
0.75% ΔF/F
25 ms
B
T462C
4% ΔF/F
25 ms

References

1. Castle, N.A., et al., *4-Aminopyridine binding and slow inactivation are mutually exclusive in rat Kv1.1 and Shaker potassium channels.* Mol Pharmacol, 1994. **46**(6): p. 1175-81.
2. McCormack, K., W.J. Joiner, and S.H. Heinemann, *A characterization of the activating structural rearrangements in voltage-dependent Shaker K+ channels.* Neuron, 1994. **12**(2): p. 301-15.
3. Bouchard, R. and D. Fedida, *Closed- and open-state binding of 4-aminopyridine to the cloned human potassium channel Kv1.5.* J Pharmacol Exp Ther, 1995. **275**(2): p. 864-76.
4. Armstrong, C.M. and A. Loboda, *A model for 4-aminopyridine action on K channels: similarities to tetraethylammonium ion action.* Biophys J, 2001. **81**(2): p. 895-904.
5. Mannuzzu, L.M., M.M. Moronne, and E.Y. Isacoff, *Direct physical measure of conformational rearrangement underlying potassium channel gating.* Science, 1996. **271**(5246): p. 213-6.
6. Cha, A. and F. Bezanilla, *Characterizing voltage-dependent conformational changes in the Shaker K+ channel with fluorescence.* Neuron, 1997. **19**(5): p. 1127-40.
7. Gandhi, C.S., E. Loots, and E.Y. Isacoff, *Reconstructing voltage sensor-pore interaction from a fluorescence scan of a voltage-gated K+ channel.* Neuron, 2000. **27**(3): p. 585-95.

8. Savalli, N., et al., *Modes of operation of the BKCa channel beta2 subunit.* J Gen Physiol, 2007. **130**(1): p. 117-31.

9. Claydon, T.W., et al., *A direct demonstration of closed-state inactivation of K+ channels at low pH.* J Gen Physiol, 2007. **129**(5): p. 437-55.

10. Loots, E. and E.Y. Isacoff, *Protein rearrangements underlying slow inactivation of the Shaker K+ channel.* J Gen Physiol, 1998. **112**(4): p. 377-89.